2

XN 8400067

NEANDC (E)-252 U Vol. V
INDC (Ger)-27/LN + Special

# PROGRESS REPORT ON NUCLEAR DATA RESEARCH IN THE FEDERAL REPUBLIC OF GERMANY

for the Period April 1, 1983 to March 31, 1984

June 1984

Edited by
S.M. Qaim

Institut für Chemie (1): Nuklearchemie
Kernforschungsanlage Jülich GmbH

NEANDC (E) [illegible] U Vol. V
INDC (Ger) [illegible]/LN + Special

# PROGRESS REPORT
# ON NUCLEAR DATA RESEARCH IN THE FEDERAL REPUBLIC OF GERMANY

for the Period April 1, 1983 to March 31, 1984

June 1984

INIS INPUT FORM

FROM: FRANCE

DATE DESPATCHED: 30/08/1985
DATE RECEIVED:

ENCLOSED PLEASE FIND INIS INPUT CONSISTING OF THE FOLLOWING MAGNETIC TAPE:

TRN OF INPUT : ( PLEASE SEE LIST ENCLOSED )

VOL.SER.NO.: FR0157
(SUITE)

TOTAL NUMBER OF ITEMS INCLUDED IN THIS INPUT :

XN : 24 -

| REPORT NO.* | ASSOCIATED TRN | REPORT NO.* | ASSOCIATED TRN |
|---|---|---|---|
| NEANDC(E)--252-U(V.5) | XN8400067 | | |

ADDITIONAL NOTES :

TRN_OF_INPUT (FR0157)

XN8400067

XN85XN019

XN85XN020

XN85XN021

XN85XN022

XN85XN023

XN85XN024

XN85XN025

XN85XN026

XN85XN027

XN85XN028

XN85XN029

XN85XN030

XN85XN031

XN85XN032

XN85XN033

XN85XN034

XN85XN035

XN85XN036

XN85XN037

XN85XN038

XN85XN039

XN85XN040

XN85XN041

---

** VEUILLEZ CADRER LE PAPIER S.V.P. ET FAIRE RETURN **

# F O R E W O R D

This report has been prepared to promote exchange of nuclear data research information between the Federal Republic of Germany and the other member states of NEA and IAEA. It brings together progress reports from KfK Karlsruhe, KFA Jülich, GKSS-Geesthacht, the Universities of Kiel, Köln, Mainz, Marburg, Stuttgart and München, as well as from PTB Braunschweig and FIZ Karlsruhe. The emphasis in the work reported here has been on measurement, evaluation and compilation of application oriented nuclear data, such as those relevant to fission and fusion reactor technologies, development of intense spallation neutron sources, production of medically important short-lived radioisotopes etc.

Each contribution is presented under the laboratory heading where the work was done. If the work is relevant to requests in the World Request List for Nuclear Data, WRENDA 81/82 (INDC(SEC)-78/URSF), the corresponding request identification numbers have been listed after the title and authors' names of the respective contribution.

Jülich, June 1984 S.M. Qaim

# CONTENTS

Page



INSTITUT FÜR NEUTRONENPHYSIK UND REAKTORTECHNIK
KERNFORSCHUNGSZENTRUM KARLSRUHE

Page

INSTITUT FÜR CHEMIE (1): NUKLEARCHEMIE
KERNFORSCHUNGSANLAGE JÜLICH



INSTITUT FÜR REINE UND ANGEWANDTE KERNPHYSIK
UNIVERSITÄT KIEL, FORSCHUNGSREAKTOR GEESTHACHT



INSTITUT FÜR PHYSIK
GKSS-FORSCHUNGSZENTRUM GEESTHACHT

Page

Page

FACHINFORMATIONSZENTRUM ENERGIE PHYSIK MATEHMATIK
KARLSRUHE

KERNFORSCHUNGSZENTRUM KARLSRUHE
INSTITUT FÜR KERNPHYSIK II

## 1. Documentation of Neutron and Charged Particle Yields and Spectra from High-Energy Proton Bombardment of Thick Heavy Metal Targets

S. Cierjacks, F. Raupp

The complete documentation of differential neutron and charged particle yields and spectra from 590 MeV and 1100 MeV proton bombardment of thick heavy metal targets measured within the feasibility study for a new German spallation neutron source (SNQ) has been finalized. While the data obtained for thick lead targets at the two incident proton energies have been documented in recent years, final results for thick uranium targets were compiled in a recent report [1]. The data are presented in tabulated and graphical form, in order to facilitate their use in subsequent work on the study, construction and operation of advanced spallation neutron sources. Absolute yield and spectra measurements presented in the report concern neutron and charged particle production from 590 MeV proton bombardment of a 10 x 10 $cm^2$, 40 cm long, uranium block. Differential data are given for three laboratory angles of $30^o$, $90^o$ and $150^o$ and five penetration depths (in steps of 5 cm) into target. Charged particle yields and spectra have been measured for secondary protons, deuterons, tritons and pions ($\pi^+ + \pi^-$).

## 2. Systematics of Angular-Dependent Neutron and Charged-Particle Production by 590 MeV protons on Thin Targets with $12 \leq A \leq 238$

S. Cierjacks, Y. Hino[1], F. Raupp

Data analyses of all neutron production cross section measurements performed in recent years at the SIN cyclotron have been completed. The results are presently used for extended intercomparisons of measurements and theoretical predictions provided by the HETC Monte Carlo code [2] (see Sect. 3). A journal publication of the experimental results of neutron production cross sections is in progress. The analysis of charged-particle production cross section measurements performed for various metal targets and several emission angles has been continued during the period covered in this report. Their final evaluation is expected to give differential production cross sections for secondary protons, deuterons, tritons and pions at five laboratory angles between $23^{\circ}$ and $157^{\circ}$ and thin metal targets of C, Al, Fe, Nb, In, Ta, Pb and U. Experimental data of this type provide valuable additional information for comparisons with theoretical predictions from modern intranuclear cascade models.

## 3. Comparisons of Measured and Calculated Differential Neutron and Charged-Particle Production Cross Sections

S. Cierjacks, Y. Hino[1], D. Filges[2], P. Cloth[2], T.W. Armstrong[2]

The systematic measurements of neutron and charged-particle production cross sections [3] (described in Sect. 2) were primarily performed in order to test the accuracy of theoretical predictions from intranuclear cascade evaporation models used in modern high-energy nucleon-meson transport codes, e.g. the HETC Monte Carlo code. In continuation of our previous work various additional total and partial production cross sections have been calculated. The previous and the new calculations now provide a complete set of cross sections which cover the whole range of measured neutron and part of the charged-particle production data [4]. Comparisons of experimental and theoretical results revealed that the neutron production cross sections in the evaporation region ($E_n \lesssim 15$ MeV) can be predicted for all targets except the very lightest (C and Al) and all emission angles with sufficient accuracy ($\sim$30%). In the cascade region, however, large discrepancies continue to persist. The differences between measurements and theoretical predictions increase with increasing emission energy and increasing emission angle. Typically the calculated cross sections at $E_n \sim 100$ MeV and emission angles in the forward direction are a factor of 2-3 lower than the measured ones. The corresponding factor increases to a value of about 10 for a backward laboratory angle of $150^{\circ}$.

---

[1] Now at Electrotechnical Laboratory, 114 Umezono, Ibaraki, Japan

[2] Institut für Reaktorentwicklung, Kernforschungsanlage Jülich, Postfach 1913, D-5170 Jülich

References

[1] F. Raupp, Messung der orts- und winkelabhängigen Spektren schneller Neutronen und geladener Sekundärteilchen aus Spallationsreaktionen von 590 MeV Protonen in dicken Urantargets, KfK-Report, KfK 3511B, Kernforschungszentrum Karlsruhe, April 1983

[2] T.W. Armstrong and K.C. Chandler, HETC - A High-Energy Transport Code, Nucl. Sci. Eng. 49 (1972) 110

[3] S. Cierjacks, Y. Hino, F. Raupp and L. Buth, Neutron and Charged-Particle Production Cross Sections for 590 MeV Protons on Thin Metal Targets with 12 $\leq$ A $\leq$ 238, in Annual Report on Nuclear Physics Activities July 1, 1982 - June 30, 1983, Eds. H. Gemmecke, F. Käppeler, Ch. Weddigen, KfK 3621, Nov. 1983

[4] D. Filges, S. Cierjacks, P. Cloth, Y. Hino and T.W. Armstrong, Validation of HETC Model Calculations for Particle Production, Joint KfK- and KFA-Report, to be published

KERNFORSCHUNGSZENTRUM KARLSRUHE
INSTITUT FÜR KERNPHYSIK III

# 1. 3 MV Van de Graaff-Accelerator

## 1.1 The Capture Width of the 34.8 keV s-Wave Neutron Resonance in $^{27}Al$*

K. Wisshak, F. Käppeler, G. Reffo+

The neutron capture width of the s-wave resonance at 34.8 keV in $^{27}Al$ has been determined using a setup with extremely low neutron sensitivity. This feature is important because this resonance exhibits a very large scattering to capture ratio. A pulsed 3-MV Van de Graaff accelerator and a kinematically collimated neutron beam, produced via the $^{7}Li(p,n)$ reaction, was used in the experiment. Capture gamma-rays were observed by three Moxon-Rae detectors with graphite-, bismuth-graphite-, and bismuth-converter, respectively. The samples were positioned at a neutron flight path of only 9 cm. Thus events due to capture of resonance scattered neutrons in the detectors or in surrounding materials are completely discriminated by their additional time of flight. The data obtained with the individual detectors were corrected for the efficiency of the different converter materials. For that purpose, theoretical calculations of the capture gamma-ray spectra of the measured isotope and of gold, which was used as a standard, were performed. The final radiative width is $g\Gamma_\gamma = 1.22 \pm 0.07$ eV. The accuracy is nearly a factor of three better than in previous experiments.

---

* submitted for publ. to Nucl. Sci. Eng.
\+ E.N.E.A., Bologna, Italy

## 1.2 Neutron Capture Cross Sections of $^{46}Ca$ and $^{48}Ca$

F. Käppeler, G. Walter, G.J. Mathews+

The neutron capture cross sections of $^{46,48}Ca$ were measured for the first time by activation of a few mg of sample material. The neutron energy spectra used in these activations peaked at 25 and 97 keV. The results obtained for $^{48}Ca$ agree very well with a 1/v-extrapolation of the thermal cross section while the $^{46}Ca$ results lie by a factor of $\sim 5$ above such an extrapolation. The cross sections are of relevance to an understanding of the origin of $^{46,48}$Ca.

---

+ University of California
Lawrence Livermore National Laboratory, USA

## 1.3 Neutron Capture in s-Wave Resonances of $^{64}$Ni*

K. Wisshak, F. Käppeler, R.L. Macklin+, G. Reffo++, F. Fabbri++

The neutron capture width of the s-wave resonances at 13.9 and 33.8 keV in $^{64}$Ni have been determined using a setup with extremely low neutron sensitivity, completely different from all previous experiments on this isotope. This feature is important because these resonances exhibit a very large scattering to capture ratio. A pulsed 3-MV Van de Graaff accelerator and a kinematically collimated neutron beam, produced via the $^{7}$Li(p,n) reaction, was used in the experiments. Capture gamma-rays were observed by three Moxon-Rae detectors with graphite-, bismuth-graphite-, and bismuth-converter, respectively. The samples were positioned at a neutron flight path of only 6-8 cm. Thus events due to capture of resonance scattered neutrons in the detectors or in sourrounding materials are completely discriminated by their additional time of flight. The short flight path and the high neutron flux at the sample position allowed for a signal to background ratio of $\sim$ 1 even for the broad resonance at 33.8 keV. The data obtained with the individual detectors were corrected for the efficiency of the different converter materials. For that purpose, detailed theoretical calculations of the capture gamma-ray spectra of the measured isotope and of gold, which was used as a standard, were performed. The final radiative widths are $\Gamma_\gamma$(13.9 keV) = 1.01 $\pm$ 0.07 eV and $\Gamma_\gamma$(33.8 keV) = 1.16 $\pm$ 0.08 eV, considerably smaller than the rough estimates obtained in previous work.

---

* KfK-report 3582, and Nucl. Sci. Eng. (in press)

+ Oak Ridge National Laboratory, USA

++ E.N.E.A., Bologna, Italy

## 1.4 Neutron Capture Cross Sections of the Krypton Isotopes and the s-Process Branching at $^{79}Se$*

G. Walter, B. Leugers, F. Käppeler, Z.Y. Bao[+], D. Erbe, G. Rupp, G. Reffo[++], F. Fabbri[++]

The input data for an analysis of the s-process branching at $^{79}Se$ have been significantly improved. The neutron capture cross sections for the stable krypton isotopes (except $^{86}Kr$) were measured between 3 and 240 keV neutron energy. In addition, statistical model calculations of the $(n,\gamma)$-cross sections for all isotopes involved in this branching were performed. With these data and with other experimental results from literature a recommended set of Maxwellian average cross sections was established in the mass region 77<A<85. The relevant decay parameters of the involved unstable nuclei and the parameters for the s-process model are discussed as well. On this basis the following aspects are investigated: the temperature during the s-process, the decomposition into s- and r-process contributions and the solar krypton abundance.

---

* KfK-report 3652 (1984)

\+ on leave from the Institute of Atomic Energy, Academia Sinica, Peking, China

++ E.N.E.A., Bologna, Italy

## 1.5 Neutron Capture Cross Sections of the Stable Xenon Isotopes and their Application in Stellar Nucleosynthesis*

H. Beer, F. Käppeler, G. Reffo[+], G. Venturini[+]

The neutron capture cross sections of $^{124,132,134}Xe$ have been measured by the activation technique at 25 keV neutron energy. These data were supplemented by calculated capture cross sections for $^{128,129,130,131}Xe$ via the statistical model, based on carefully evaluated local parameter systematics. The complete set of capture cross sections obtained in this way is shown in Table I together with previous, more global calculations. The uncertainty of our theoretical results is estimated to be 20 %.

Table I Comparison of the Xenon Cross Sections Obtained in this Work with Various Calculations at kT = 30 keV

| Xe-Isotopes | $\sigma_{n\gamma}$ (mb) | | | | | |
|---|---|---|---|---|---|---|
| | Harris (1) | Holmes et al.(2) | ENDF/B-V (3) | Benzi et al.(4) | present work calc. | present work exp. |
| 128 | 510 | 232 | 206 | 239 | 249 | |
| 129 | 1454 | 666 | 560 | 572 | 470 | |
| 130 | 207 | 143 | 156 | 189 | 153 | |
| 131 | 570 | 587 | 310 | 491 | 348 | |
| 132 | 74.9 | 91 | 85 | 116 | 65 | $61\pm4$ |
| 134 | 37.5 | 47.5 | 41 | 60 | 33 | $29\pm2$ |

With these cross sections we determined the solar xenon abundance through s-process systematics and decomposed the abundances of $^{129,131,132}$Xe into their s- and r-process contributions. Furtheron, various isotopic anomalies in the xenon isotopes, which were detected in several meteorites, are discussed in detail.

(1) M.J. Harris, Astrophys. Space Sci. 77 (1981) 357
(2) J.A. Holmes, S.E. Woosley, W.A. Fowler, B.A. Zimmerman, At. Data and Nucl. Data Tables 18 (1978)
(3) Kinsey, ENDF/B Summary Documentation, BNL-NCS-17541 (1979)
(4) V. Benzi, R.D'Orazi, G. Reffo, M. Vaccari, CNEN-report RT/FI6 (1972)

---

* Astrophysics and Space Science 97 (1983) 95

+ E.N.E.A., Bologna, Italy

## 1.6 Neutron Capture Nucleosynthesis of Neodymium Isotopes and the s-Process from A = 130 to 150 *

G.J. Mathews+, F. Käppeler

New measurements of neutron capture cross sections for $^{142,143,144}$Nd are reported. These are combined with other recent measurements and applied to a detailed study of the s-process and r-process systematics for A = 130 to 150 nuclei. The influence of these results on the interpretation of isotopic

---

* submitted to the Astrophysical Journal

+ University of California, Lawrence Livermore National Laboratory, USA

anomalies observed in acid insoluble residues and inclusions from the Allende meteorite is also examined. The uncertainties in the s-process $\sigma N$ curve are significantly diminished in the present work and a fit is obtained which is consistent with all of the s-process-only isotopes in this region. A somewhat larger value than previous determinations is obtained for the mean neutron exposure for heavy nuclei in the s-process, $\tau_0 = 0.29 - 0.35\ mb^{-1}$. The derived r-process abundances decrease systematically from the A = 130 peak but exhibit a pronounced odd-even effect. The new results tend to confirm the hypothesis that the isotopic anomalies in materials from the Allende meteorite are the result of an unusual mixture of average solar-system s-process and r-process material, but a previously unobserved odd-even effect may be present in the r-process anomalies of inclusion EK1-4-1.

## 1.7 The s-Process Branching at $^{151}Sm$*

H. Beer, F. Käppeler, K. Yokoi+, K. Takahashi+

The s-process branching in the mass region $150 \leq A \leq 154$, initiated by the $^{151}Sm$ $\beta^-$ decay, is reinvestigated, particularly in connection with the solar $^{152}Gd$ abundance. The Maxwellian averaged neutron capture cross sections for kT = 25 keV are measured for $^{152}Sm$, $^{151}Eu$ (to the 9.3 hour isomeric state of $^{152}Eu$), $^{152}Gd$, $^{158}Gd$, and $^{160}Gd$. The ß-decay rates of the unstable nuclei involved in the branching are calculated theoretically. In addition, it is shown that the thermal equilibration between the ground state and the isomeric state in $^{152}Eu$ under plausible s-process conditions is achieved on a time scale shorter than those for ß-decay and neutron capture. With these results and the neutron capture cross sections from literature for the other concerned nuclei, a branching analysis is performed within the steady flow model of the s-process. This study yields constraints for s-process models, particularly with regard to temperature and neutron density.

---

* The Astrophysical Journal 278 (1984) 388

\+ Technische Hochschule Darmstadt

## 1.8 Self-Absorption of Neutron Capture Gamma-Rays in Gold Samples*

K. Wisshak, G. Walter, F. Käppeler

The self absorption of neutron capture gamma-rays in gold samples has been determined experimentally for two standard setups used in measurements of neutron capture cross sections. One makes use of an artificially collimated neutron beam and two $C_6D_6$ detectors, the other of kinematically collimated neutrons and three Moxon-Rae detectors. With a gold sample of 1 mm thickness correction factors up to 12 % were found for an actual neutron capture cross section measurement using the first setup while they are only 4 % for the second setup. The present data allow to determine the correction in an actual measurement with an accuracy of 0.5 - 1 %.

---

* Nucl. Instr. Meth. 219 (1984) 136

## 1.9 Large Barium Fluoride Detectors*

K. Wisshak, F. Käppeler

Large $BaF_2$ crystals of 1 - 2 l volume and up to 15 cm thickness were investigated with respect to their application as gamma-ray detectors. In particular, we were interested in the light transmission in the UV region, and the energy and time resolution. We found that an energy resolution of ∿ 12 % (662 keV) and a time resolution of ∿ 0.4 ns ($^{60}Co$, 300 keV threshold) can be obtained simultaneously. For these features $BaF_2$ is superior to NaI or BGO in cases where good timing is essential. Gamma-rays and alpha particles can be clearly discriminated, as for the latter the fast component does not show up in the scintillation light.

---

* Nucl. Instr. Meth. (in press)

## 1.10 Calculated Efficiency of a $4\pi$ Detector of BGO or $BaF_2$ for Monoenergetic Gamma Rays and Gamma Cascades Following Neutron Capture*

K. Wisshak, F. Käppeler, G. Schatz

The applicability of a spherical shell of BGO or $BaF_2$ as a $4\pi$ detector for high precision measurements of neutron capture cross sections was investigated. Firstly, the efficiency of both scintillator materials for monoenergetic gamma rays was calculated in the energy range from 0.5 to 10 MeV. Configurations with different thickness and inner radii were considered. Secondly, neutron capture cascades were calculated for several isotopes with widely different capture gamma ray spectra according to the statistical model. Both informations together allowed to determine the efficiency of an actual detector for neutron capture events in dependence of the threshold energy. A thickness of 10 cm BGO or 17.5 cm $BaF_2$ proved to be sufficient to register more than 95 % of all capture events above a threshold energy of 3 MeV. This reduces the systematic uncertainty due to the detector efficiency in an absolute cross-section measurement to less than 1 % and in a relative measurement using a gold standard to less than 0.5 %.

---

* Nucl. Instr. Meth. 221 (1984) 385

KERNFORSCHUNGSZENTRUM KARLSRUHE
INSTITUT FÜR NEUTRONENPHYSIK UND REAKTORTECHNIK

## 1. Nuclear Data Evaluation

### 1.1 Neutron Data for Fusion Applications

B. Goel, I. Broeders, U. Fischer, H. Jahn, B. Krieg,
H. Kuesters, M. Segev, E. Stein, E. Wiegner

(Relevant to request numbers 724007F, 724008F, 732004F, 762246F, 821046F ,832036F, 832002F, 792112R, 781222F, 832043F, 724058F, 792023F, 801021F)

Reliable nuclear data for fusion are becoming more and more important as operation of facilities such as the Joint European Torus (JET), design studies for its successor (NET) and increasingly detailed conceptual studies of fusion reactors and fission-fusion hybrids create data demand for the calculation of activation, radiation damage, shielding, tritium breeding etc. Our recent activities were concentrated on

a) assessment of the relevant cross sections in the evaluated neutron data file KEDAK which at present contains mainly neutron cross sections for fission reactor calculations,

b) participation in a benchmark exercise concerning theoretical models and codes for pre-equilibrium reactions,

c) critical analysis of Pb(n,2n) cross section data.

During the HIBALL study (heavy-ion induced fusion with inertial confinement, [1]) the $^{7}$Li(n,n't) cross section was evaluated at KfK on the basis of then available "new" experiments and of the integral tritium-breeding experiment performed here [2]. The result of this evaluation together with another evaluation from Los Alamos [3] and the recent experimental data [4-7] are displayed in Fig. 1. At the time of our evaluation only preliminary data from Geel were available. In the region around 6 MeV our evaluation is a bit higher than the final Geel-Jülich data (Liskien et al.) but well within the experimental uncertainties. The Harwell data (Swinhoe and Uttley) in Fig. 1 are consistently lower than the evaluations and other experimental data. Revised Harwell data [8] obtained with more precise multiple scattering corrections are about 3-6 % higher than those reproduced in Fig. 1. The accuracy of our evaluation is about 7 % . This may be regarded as sufficient, especially because in most recent blanket designs the $^7Li(n,n't)$ process contributes only a few percent to the total breeding ratio. Only in the case of a Li or $Li_2O$ blanket is a higher accuracy required. In some of the blanket designs the use of $ZrH_x$ is proposed [9]. KERMA factors for both Zr and H are missing in the data base used. To make up for this deficiency we have implemented the MACK-IV code [10] at KfK and will use it to generate KERMA factors.

For the treatment of precompound processes in nuclear reactions we have modified our version of the HAUSER*4 code [11] so as to allow simultaneous generation of (n,n') and (n,2n) neutron emission spectra. The pre-equilibrium contribution is calculated with the geometry-dependent hybrid model [12]. As shown in Fig. 2, experimental data for $^{93}Nb$ are well reproduced with this code system. It should be noted that these benchmark results including the pre-equilibrium part are computed exclusively from the optical model, without adjustment of special pre-equilibrium parameters such as the squared matrix element required in the exciton model. In the high-energy tail observed in emission spectra induced by 14 MeV neutrons the calculated results are still within the very large error bars of the data. The role of collective excited states in this part of the emission spectrum requires further study.

In the neutron multiplication experiment on Pb by Takahashi et al. [13] more neutrons were observed than predicted with ENDF/B-V data. Another experiment by Aleksandrov et al. [14] leads to the same conclusion. These observations are in conflict with the (n,2n) cross section measurement by Frehaut et al. [15]. A critical analysis of the Takahashi results reveals that they imply 13 % of the Pb(n,2n) neutrons to remain above the (n,2n) threshold. This is kinematically highly improbable. Therefore the experiment should be reinvestigated.

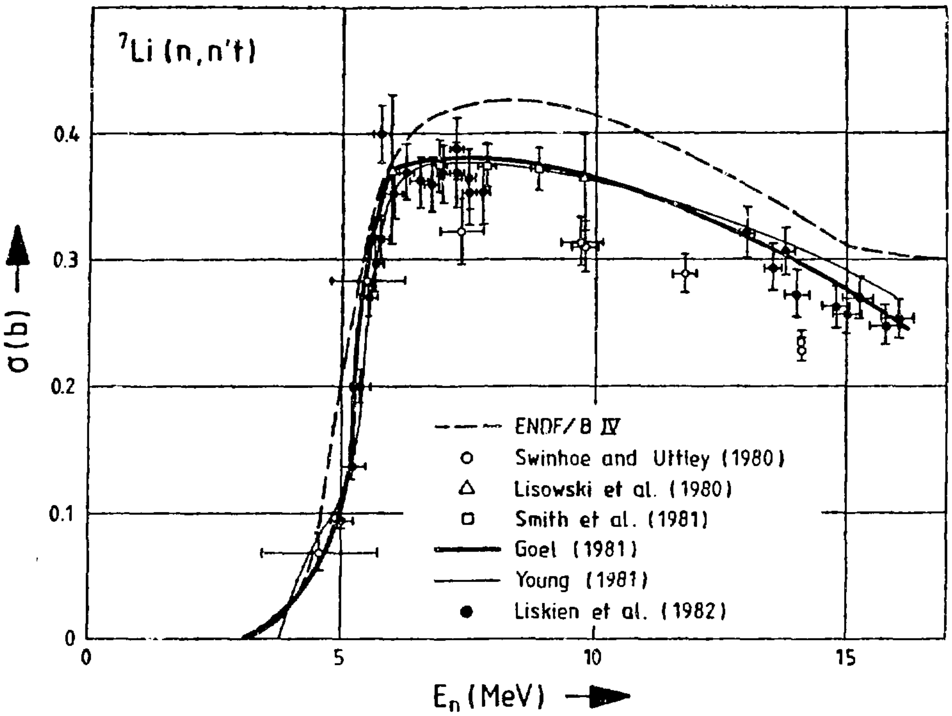


Fig. 1 $^7$Li(n,n't) cross section: comparison of evaluations (curves) and measurements (points).

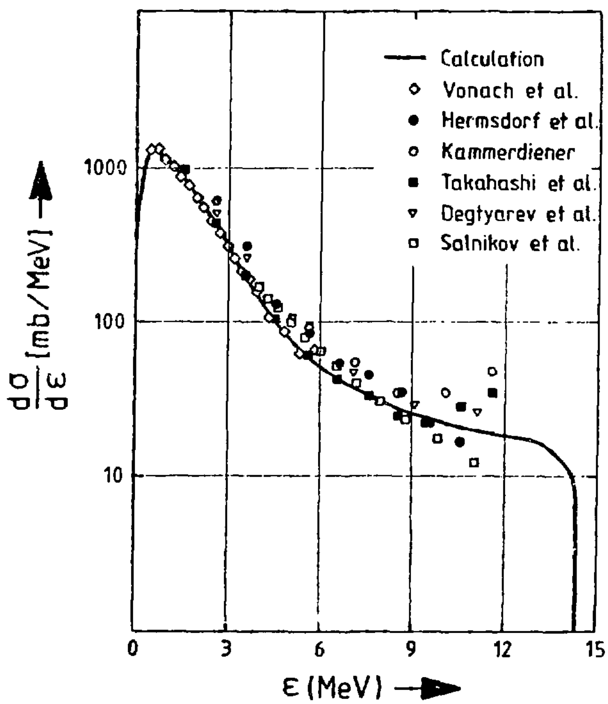


Fig. 2 Neutron emission spectrum for $^{93}$Nb. The curve was calculated with the geometry-dependent hybrid model, based only on optical model quantities (no fit of precompound parameters). The points are measured values.

References

[1] HIBALL, KfK 3202/1+2 (1981)

[2] H. Bachmann et al., Nucl. Sci. Eng. 67 (1978) 74

[3] P.G. Young, LA-8874-PR (1981) p. 2

[4] M.T. Swinhoe and C.A. Uttley, AERE-R 9929 (1980)

[5] P.W. Lisowski et al., LA-8342 (1980)

[6] D. L. Smith et al., Nucl. Sci. Eng. 78 (1981) 359

[7] H. Liskien et al., Proc. Int. Conf. on Nucl. Data for Sci. and Technol. Antwerp 1982, Dordrecht (1983) p. 349

[8] M.T. Swinhoe, private communication (1984)

[9] M. Dalle Donne et al., KfK 3584 (1983)

[10] M.A. Abdou, ANL/FPP-77-5

[11] U. Fischer, KfK 2907 (1980);
B. Goel and F.H. Fröhner, Proc. 12th Int. Symp. on Nucl. Physics, Gaussig 1982, ZfK 491 (1982) p. 180

[12] H. Jahn, Proc. Int. Conf. Nucl. Data for Reactors, Harwell (1978) p. 502

[13] A. Takahashi et al., Symp. Fusion Technol., Jülich 1982

[14] V.D. Aleksandrov et al., At. En. 52 (1982) 422, translation KfK-tr-682 (1982)

[15] J. Fréhaut et al., Symp. Neutron Cross Sections from 10-50 MeV, Brookhaven 1980, BNL-NCS-51245 (1980) vol. 1, p. 399

# 2. Nuclear Reaction Theory

## 2.1 Investigation of Precompound Reaction Models

H. Jahn

(Relevant to request numbers 692100F, 702007R, 714004R, 761075R, 781048F, 832025F, 832042F, 742129R, 792112R, 781222F, 832043F)

The predictive capability of most precompound models that are presently available is limited by too much arbitrariness in the choice of parameters. The origin of this arbitrariness was recently analysed in detail in a review of available precompound descriptions and their performance in the light of experimental data [1]. The main contestants are the exciton model on one hand and the hybrid model on the other.

The exciton model introduced by Cline and Blann [2] is based on the master equations, a system of balance equations for transitions between states with different numbers of particles and holes (excitons). Despite this formally appealing approach it is beset by difficulties concerning e. g. the pairing corrections to particle-hole as well as compound state densities, and especially by a lack of theoretical understanding of the effective matrix element that governs creation and annihilation of particle-hole pairs. The universality of its assumed mass and energy dependence is in serious doubt. Large excursions are observed from the postulated smooth trend, and attempts to blame them on shell effects were not very successful since nuclei between closed shells are afflicted too. Another ambiguity, about the Pauli correction in the transition state densities, could recently be removed by Anzaldo [3] who used number theory to derive its correct form. Calculations of the transition rates from nucleon-nucleon scattering in nuclear matter gave values which were 4 to 10 times too low. Apparently direct processes are not included at all in the present form of the exciton model. Since its predictive power is thus severely limited its usefulness is restricted to data fitting and inter- or extrapolation over limited energy ranges.

Blann overcame many of the difficulties of the exciton model by means of an "intermarriage" [4] between the exciton master equation [2] and the

Harp-Miller-Berne equation [5]. The influence of the diffuseness of the nuclear surface turned out to be important and led from the original hybrid model to the geometry-dependent hybrid model. Its optical-model version contains, apart from general nuclear parameters such as the nucleon numbers N and Z, only optical-model quantities, in particular the nuclear radius, the surface diffuseness, the imaginary well depth and the cross section for compound nucleus formation. It is the only existing model that takes the diffuseness of the nuclear surface into account. Furthermore, its 3-exciton ($n_0 = 3$) component includes the clearly geometry-dependent statistical direct processes as Blann indicated and as its relationship to the Harp-Miller-Berne theory [5] suggests which latter is known to include the statistical direct reactions. Consistent with this we find that the geometry-dependent hybrid model describes, without fit, the $^{56}$Fe data on double-differential neutron scattering at 7.54 and 14.6 MeV incident energy quite well, and is in good agreement with angle-integrated DWBA results at 14.6 MeV. Similarly good agreement between measured data and calculations with the geometry-dependent hybrid model was found for $^{55}$Mn and $^{93}$Nb.

References

[1] H. Jahn, Lecture Notes, ICTP Trieste, Jan.-Feb. 1982, IAEA-SMR-93; KfK 3646 (1984)

[2] C.K. Cline and M. Blann, Nucl. Phys. A172 (1971) 225

[3] A.M. Anzaldo Meneses, Proc. IAEA Meet. on Basic and Appl. Problems of Nucl. Level Densities, Brookhaven 1983, BNL-NCS-51694 (1983) 91

[4] M. Blann, Ann. Rev. Nucl. Sci. 25 (1975) 123

[5] G.D. Harp, J.M. Miller, B.J. Berne, Phys. Rev. 165 (1968) 1166; Phys. Rev. C3 (1971) 1847

## 2.2 Statistical Distributions of R-matrix Elements and Cross Sections

F.H. Fröhner

The problem of resonance-averaged partial cross sections (width fluctuation factors) has recently been reinvestigated in the context of the statistical model with information-theoretical methods such as entropy maximisation and analytic ergodicity. For pure scatterers the S-matrix reduces to a simple phase factor, $U = \exp(i\theta)$, and the phases are found to be distributed according to

$$p(\theta)d\theta = \mathrm{Re}\left(\frac{e^{i\theta}+\langle U\rangle}{e^{i\theta}-\langle U\rangle}\right)\frac{d\theta}{2\pi}\,, \qquad -\pi<\theta\leq\pi\,,$$

where the expectation value $\langle U\rangle$ is the resonance-averaged (optical-model) S-function. This result, given in less compact form by Lopez et al. [1], follows directly from the fact that causality requires all S-matrix poles to lie below the real axis in the complex energy plane. Using the relationship between S- and R-matrix and expressing $\langle U\rangle$ in terms of the pole strength function s and the distant-level parameter $R^{\infty}$ one finds that the R-function values obey a Cauchy distribution around the distant-level parameter, with a width proportional to the strength function,

$$p(R)dR = \frac{s\,dR}{(R-R^{\infty})^2+\pi^2 s^2}\,, \qquad -\infty<R<\infty\,.$$

We note that the formal dependence on the R-function parameters (resonance energies and reduced widths) and their frequency distributions (Gaussian orthogonal ensemble distribution and Porter-Thomas distribution, respectively) are the same for the R-function of the single-channel case as for the diagonal elements $R_{cc}$ of the general multi-channel case. Thus the $R_{cc}$ obey analogous Cauchy distributions, with the appropriate strength functions $s_c$ and distant-level parameters $R_c$. The cross section distribution for a pure scatterer is also readily derived as

$$p(\sigma)d\sigma = \frac{1}{\pi\sin\theta}\,\mathrm{Re}\left(\frac{e^{i\theta}+\langle U\rangle}{e^{i\theta}-\langle U\rangle}+\frac{e^{-i\theta}+\langle U\rangle}{e^{-i\theta}-\langle U\rangle}\right)\frac{d\sigma}{4\pi\lambda\!\!\!^{-2}}\,, \qquad 0\leq\sigma\leq4\pi\lambda\!\!\!^{-2}$$

with $\qquad \theta = \left|\arccos\left(1-\frac{\sigma}{2\pi\lambda\!\!\!^{-2}}\right)\right|\,,$

and $\qquad \langle U\rangle = e^{-2i\phi}\,\frac{1-(R^{\infty}+i\pi s)L^{o*}}{1-(R^{\infty}+i\pi s)L^{o}}\,.$

This result should be useful for applications such as sample thickness corrections to resonance-averaged transmission data and the preparation of probability tables for Monte Carlo or multi-band self-shielding calculations, as long as elastic scattering is the dominant reaction. Fig. 3 shows s-wave cross section distributions for $^{56}Fe$ below the first inelastic threshold calculated in this way.

## Reference

[1] G. Lopez, P.A. Mello, T.H. Seligman, Z. Physik A302 (1981) 351

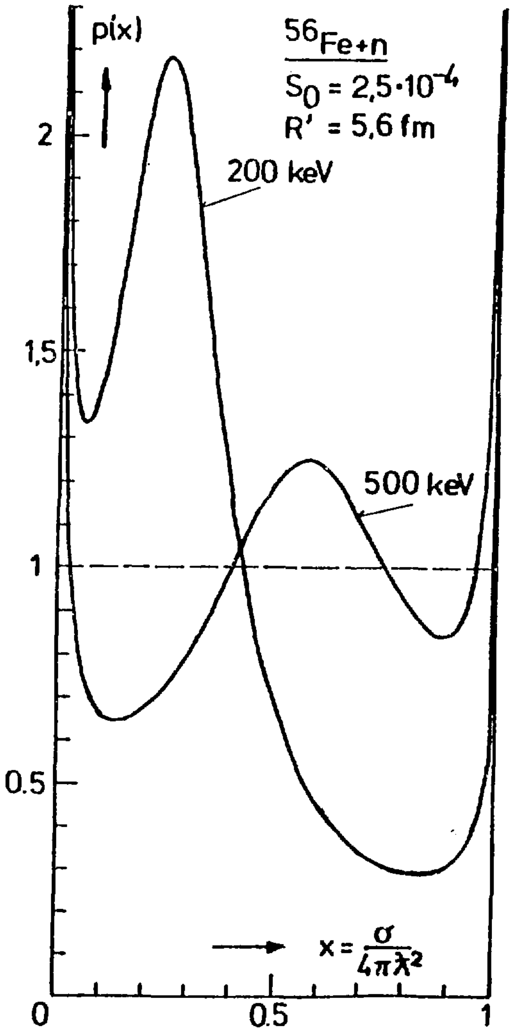


Fig. 3 Frequency distribution of the total neutron cross section for $^{56}Fe$ at two energies below the first inelastic threshold. The peaks correspond to the potential-scattering cross section.

INSTITUT FÜR CHEMIE (1): NUKLEARCHEMIE

KERNFORSCHUNGSANLAGE JÜLICH

# 1. Neutron Data

## 1.1 Study of (n,t) Reactions

S.M. Qaim, G. Stöcklin, R. Wölfle

In continuation of our radiochemical studies on fast-neutron induced trinucleon emission reactions [cf. 1] we completed our measurements on (n,t) reactions induced by 3o MeV d(Be) break-up neutrons [2]. The neutron spectrum was characterized by the multiple foil activation technique using various threshold reactions; for unfolding the iterative code SAND II was used. Tritium was separated from each irradiated sample by vacuum extraction and counted in the gas phase using a low-level $\beta^-$ detector. The measured cross sections are given in Fig. 1 as a function of Z of the target element. The trend is similar to that with a 53 MeV d(Be) break-up neutron spectrum reported previously from our laboratory. Apart from the initial decrease, the cross section is almost constant over the entire range of Z = 22 to 83. This observation suggests that triton emission from medium and heavy mass nuclei (A = 48 to 2o9) occurs via surface reactions. In order to shed some light on reaction mechanism, HauserFeshbach calculations were performed. The calculated data are also shown as a trend in Fig. 1. The smooth curve drawn through the experimental points and the theory agree within a factor of 2 in the region of Z = 13 to 2o. It appears that the (n,t) cross section of nuclei in the (2s,1d) shell is described by the statistical model. For heavier nuclei, however, non-

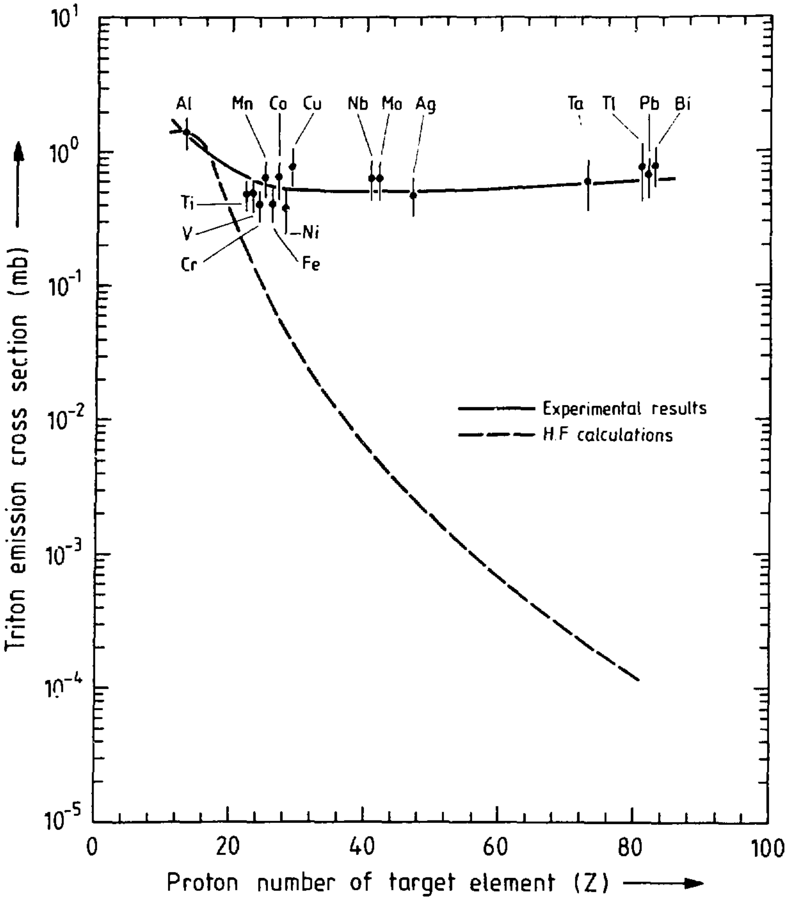


Fig. 1 Systematics of triton emission cross sections with 3o MeV d(Be) break-up neutron spectrum. The results of Hauser-Feshbach calculations are shown as a trend [2].

statistical processes appear to be more important.

## 1.2 Cross-Section Measurements of Neutron Threshold Reactions in the Energy Region of 5 to 1o MeV

S.M. Qaim, M.M. Rahman, R. Wölfle

(Relevant to request identification numbers: 692159 R, 7o2o1o R, 724o55 F, 722148 F, 722149 F, 724o56 F, 732o32 F, 732o44 R, 752244 F, 7621o7 F, 7621o8 F, 76213o F, 762242 F, 7922o9 R, 79211o R, 79221o R)

A deuterium gas target was used to produce quasi-monoenergetic neutrons via the reaction $^{2}H(d,n)^{3}He$ at our compact cyclotron. By varying the energy of the incident deuteron beam between 3 and 7 MeV, neutrons of energy between 5 and 1o MeV are obtained in the $0^{o}$ direction. Some of the characteristics of this neutron source were investigated. The neutron spectrum was characterized by the multiple foil activation technique in combination with the iterative code SAND II, and the results were qualitatively similar to those from time of flight measurements. Using this neutron source cross-section measurements on some isotopes of nickel, mentioned in last year's report, were completed. Use was made of the activation technique, wherever necessary radiochemical separations, and X- or γ-ray counting. The results for (n,α) reactions are given in Fig. 2 [cf. 3]. Cross sections were also measured for (n,p) reactions on $^{61}Ni$ and $^{62}Ni$.

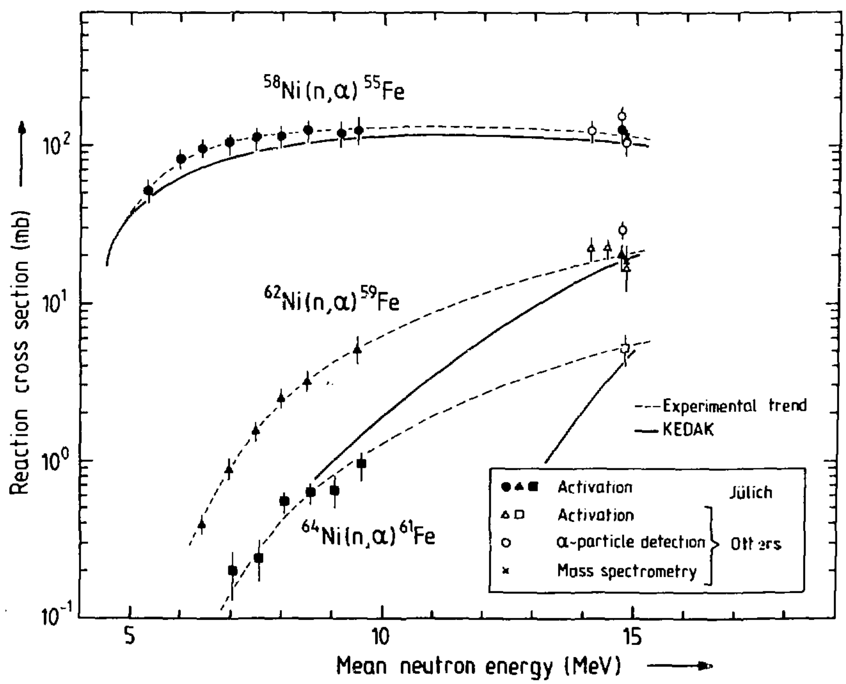


Fig. 2 Excitation functions of (n,α) reactions on $^{58}Ni$, $^{62}Ni$ and $^{64}Ni$. The broken lines give experimental trends and the solid lines KEDAK values [3].

Molybdenum is a potential constituent of the first wall of a fusion reactor. The cross-section data base for this element was, however, found to be rather weak. We therefore started measurements on $^{92,95,96,97,98}Mo(n,p)$, $^{92,98}Mo(n,\alpha)$ and $^{100}Mo(n,2n)^{99}Mo$ reactions. Statistical model analysis of the data is in progress.

## 2. Charged Particle Data for Radioisotope Production

Z. Kovacs, S.M. Qaim, G. Stöcklin

In continuation of our studies [cf. 4-6] on the production of medically important short-lived radioisotopes, excitation functions of some nuclear reactions relevant to the production of $^{117m}Sn$ and $^{75}Br$ were measured.

As discussed in last year's report, $^{117m}Sn$ is a potentially important radioisotope for single photon emission computed tomography (SPECT). Studies on the four potentially useful reactions, viz. $^{nat}Cd(\alpha,xn)^{117}Sn$, $^{nat}Cd(^{3}He,xn)^{117m}Sn$, $^{nat}In(\alpha,pxn)^{117m}Sn$ and $^{nat}In(^{3}He,pxn)^{117m}Sn$, were completed [7]. The data for the α-particle induced reactions on indium are shown in Fig. 3.

From the excitation functions and thick target yields the $^{116}Cd(\alpha,3n)^{117m}Sn$ and $^{115}In(\alpha,pn)^{117m}Sn$ reactions appear to be most promising for the production of $^{117m}Sn$.

$^{75}Br$ ($T_{1/2}$ = 1.6 h) is a positron emitter and has found application in positron emission computed tomography (PECT). The various nuclear processes used for its production have been recently reviewed [6]. The two major production methods make use of the $^{75}As(^{3}He,3n)^{75}Br$ and

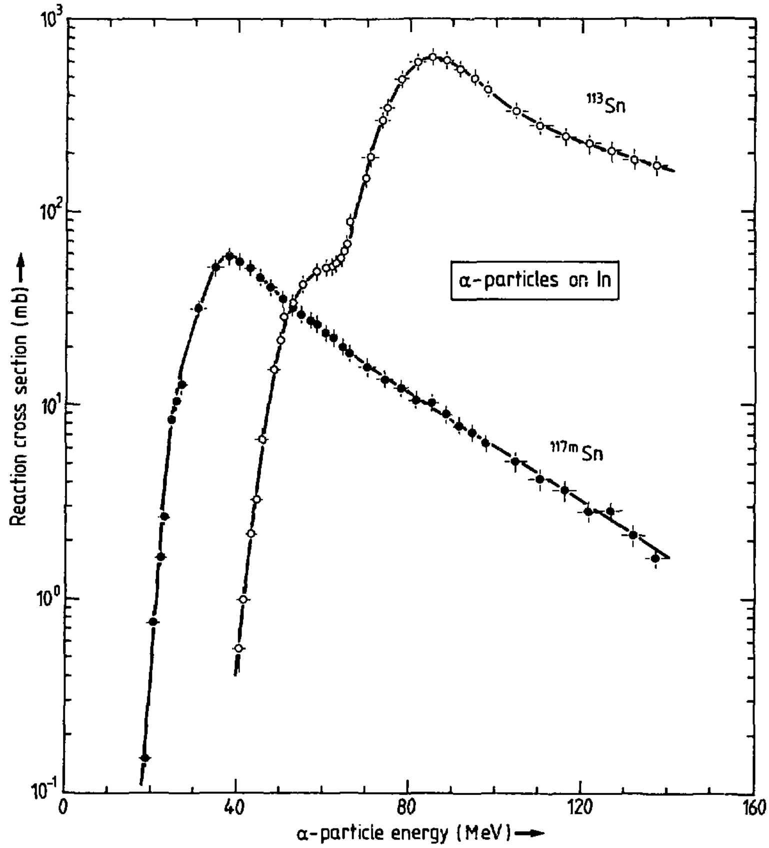


Fig. 3 Excitation functions for the formation of $^{113}Sn$ and $^{117m}Sn$ in the interactions of α-particles on natural indium [7].

$^{76}Se(p,2n)^{75}Br$ reactions. The cross-section data of the latter reaction, reported by the Groningen group, needed re-investigation. We made thin samples by electrodeposition of 96.5 % enriched $^{76}Se$ on Al and measured the excitation functions of the (p,n) and (p,2n) reactions up to 4o MeV by the stacked-foil technique. A more detailed analysis of the data is in progress.

References


[1] S.M. Qaim, C.H. Wu, R. Wölfle, $^{3}$He-particle emission in fast neutron induced reations, Nucl. Phys. A 41o (1983) 421

[2] R. Wölfle, S. Khatun, S.M. Qaim, Triton emission cross sections with 3o MeV d(Be) break-up neutrons, Nucl. Phys. A 423 (1984) 13o

[3] S.M. Qaim, R. Wölfle, M.M. Rahman, H. Ollig, Measurement of (n,p) and (n,$\alpha$) reaction cross sections on some isotopes of nickel in the energy region of 5 to 1o MeV using a dd gas target at a compact cyclotron, Nucl. Sci. Eng., in press

[4] R. Weinreich, J. Knieper, Production of $^{77}$Kr and $^{79}$Kr for medical applications via proton irradiation of bromine: Excitation functions, yields and separation procedure, Int. J. appl. Radiat. Isotopes 34 (1983) 1335

[5] J.H. Zaidi, S.M. Qaim, G. Stöcklin, Excitation functions of deuteron induced nuclear reactions on natural tellurium and enriched $^{122}$Te: Production of $^{123}$I via the $^{122}$Te(d,n)$^{123}$I-process, Int. J. appl. Radiat. Isotopes 34 (1983) 1425

[6] S.M. Qaim, G. Stöcklin, Production of some medically important short-lived nuetron deficiènt radioisotopes of halogens, Radiochimica Acta 34 (1983) 25

[7] S.M. Qaim, H. Döhler, Production of carrier-free $^{117m}$Sn, Int. J. appl. Radiat. Isotopes, in press

Institut für Reine und Angewandte Kernphysik
Universität Kiel, Forschungsreaktor Geesthacht*

## Fast-Chopper Time-of-Flight Spectrometer

H.-G. Priesmeyer, B. Asmussen, P. Fischer, U. Harz, P. Henkens

### 1. Transmission Measurements using the 24 keV-Ironfilter

The ironfilter - described in the last report - has been used to measure the total cross section of elemental lead, cadmium and gold. We find the following values in good agreement with BNL 325 data:

| | |
|---|---|
| Pb: | 10.8 ± 0.1 barn |
| Cd: | 6.9 ± 0.2 barn |
| Au: | 13.3 ± 0.2 barn |

For the measurements the titanium filter-difference method was used. The high-energy neutron contamination, which is now assumed to be about 2 % of the total neutron intensity, will be determined more precisely by a high-resolution transmission measurement of the filter itself to be performed in the near future.
An experiment to determine the n,p total cross section on hydrogen gas for calibration purposes is in progress.

### 2. Resonance Parameters of the 5.4 eV Level in Dy-162

Request 82047 of the NNDC Compilation of Request for Nuclear Data is for better parameters of the 5.4 eV Dy-162 resonance, which is well in the range of the Kiel Fast-Chopper facility. Therefore very thin samples have been prepared to be able to investigate this rather intensive level. A 20 μ thick metallic natural dysprosium film evaporated on aluminium has been used to perform a measurement at 77 K in order to study the resonance shape with reduced Doppler broadening. The preliminary results achieved for an n = 0.000101 at/b-sample using natural $Dy_2O_3$, dissolved in 10 ml $HNO_3$ and diluted in 100 ml $D_2O$, are the following:

$$E_o = 5.45 \text{ eV}$$
$$\Gamma_n^o = 12 \text{ meV}$$
$$\Gamma^n = 112 \text{ meV}$$

There is no indication of a resonance doublet, as can be seen from Fig. 1. Final resonance paremeters will be presented after a concluding experiment on a sample containing Dy-162 with 92.39 % enrichment.

## 3. Resolution Function and Transmission of the Kiel Fast-Chopper Spectrometer

In order to improve the results of resonance shape analysis of the chopper measurements, an effort has been undertaken to determine the resolution function of the spectrometer to a higher accuracy. Completed up to now is a Monte-Carlo calculation in two dimensions for a "black" and a "grey" rotor/collimator system. The neutron transmission, i.e. especially critical and cut-off energies, is also calculated. Experimental verification of the theoretical results is underway.

## 4. Publications

Priesmeyer: Bibliographie "Kalte Neutronenquelle", Stand April 1983, GKSS 83/I/24

Harz, Fischer, Priesmeyer: Ein modernes System zur Messung und Auswertung von Neutronenflugzeitspektren. Conf. "Frühjahrstagung, Kernphysik", Münster 1983, DPG Verhandlungen S. 1097

Priesmeyer: Ein fokussierender Leiter für langsame Neutronen, Münster 1983 ibid, S. 1097

Henkens, Fischer, Harz, Priesmeyer: Ein 24-keV Neutronenfilter am FR Geesthacht I, Münster 1983 ibid, S. 1111

Priesmeyer: Computational investigations of a catenary-shaped double-reflecting neutron guide, GKSS 83/E/53

Fischer, Harz, Priesmeyer: Total neutron cross section of the proton bound in zirconium hydride at low temperature, ATKE/Kerntechnik 43(1983) 294

Priesmeyer: Sequentielle Analyse der Daten eines Monitors für radioaktive Strahlung, GKSS 84/E/3

Fischer, Harz, Priesmeyer: Die Resonanzparameter der Dysprosium 162 bei 5.4 eV, Conf. "Frühjahrstagung Kernphysik", Innsbruck 1984, DPG-Verhandlungen S. 923

Asmussen, Fischer, Harz, Priesmeyer: Auflösung und Transmission eines Fast-Chopper-Flugzeitspektrometers, Conf. "Frühjahrstagung Kernphysik", Innsbruck 1984, DPG-Verhandlungen S. 1037

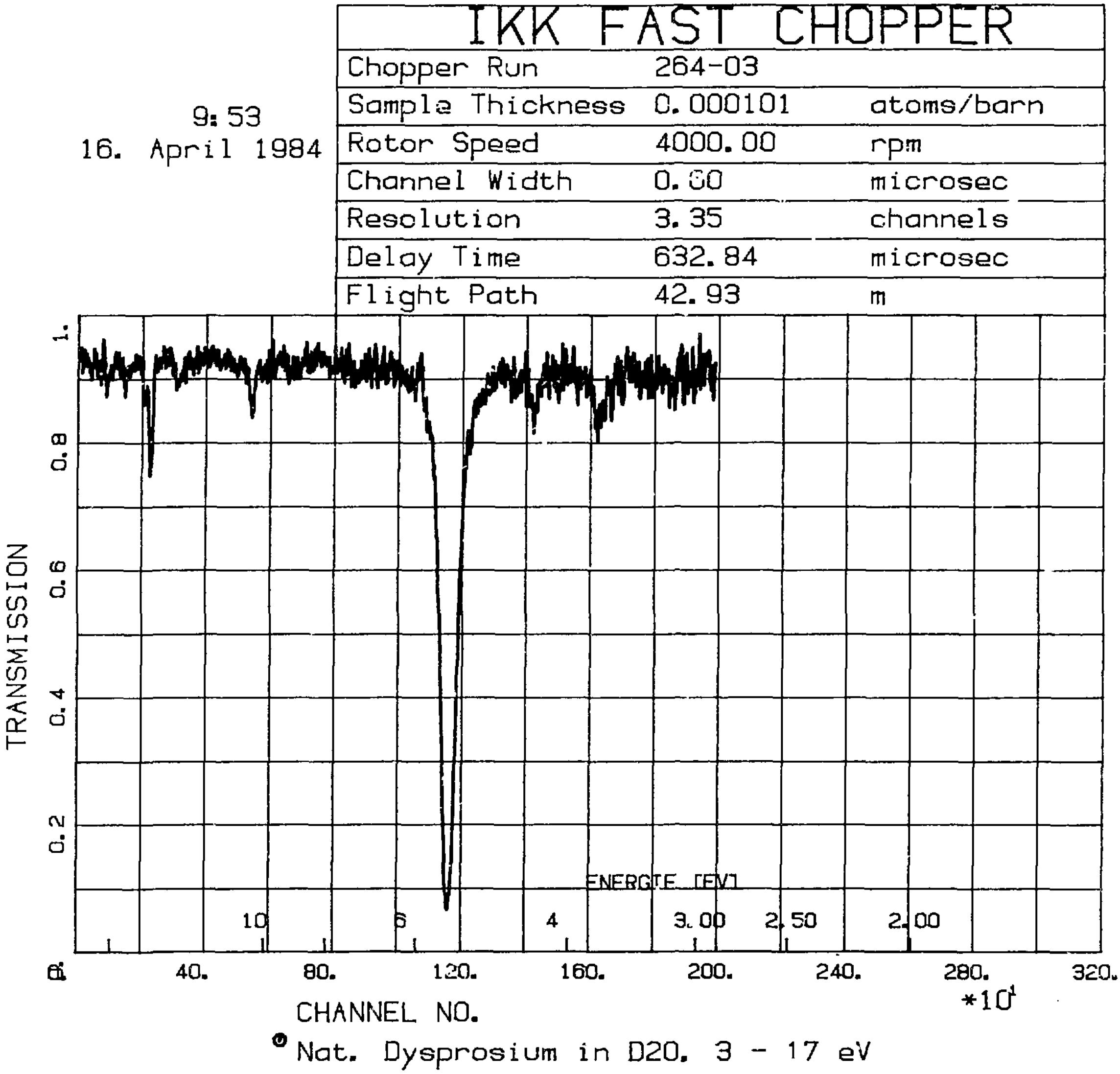


Fig. 1 Transmission of natural dysprosium, diluted in heavy water.

INSTITUT FÜR PHYSIK

GKSS-FORSCHUNGSZENTRUM GEESTHACHT

## 1. Neutron Generator Facility KORONA

R. Pepelnik, B. Anders, H.-U. Fanger, W. Michaelis

### 1.1 KORONA - a Neutron Generator combined with a Fast Rabbit System

At the GKSS Research Center Geesthacht a new intense 14 MeV neutron generator is in operation since 1981. The main components of the facility, named KORONA, are a sealed neutron tube and an integrated fast pneumatic rabbit system [1]. The neutron tube with a cylindrical acceleration structure was developed by Schmidt [2] for radiotherapy purposes. In order to meet the requirements for 14 MeV neutron activation analysis the interior space of the closed-end neutron tube had to be made accessible for a fast sample transfer system. A neutron flux of more than $3 \times 10^{10}$ n/cm$^2$s can be produced via the T(d,n)-reaction in the center of the cylindrical neutron generator target.

Solid as well as liquid samples can be irradiated in polyethylene containers with volumes of 0.55 ccm. The activated samples are pneumatically transferred to a 16 m distant detector station within 140 ms. For the investigation of short-lived radioisotopes cyclic activation is feasible.

The γ-ray spectroscopy system consists of a 93 ccm Ge(Li)detector, a Canberra-2001 preamplifier, a Canberra-2020 main amplifier, a Laben-8215 ADC and a Nuclear Data-66 MCA. Due to the high source strength of the generator, high initial activities of short-lived isotopes are induced with more than $10^6$ Bq, typically. At maximum rates of $8 \times 10^5$ cps, counting losses of 99 % occur. Therefore, the γ-ray spectroscopy system has been improved considerably with regard to the capability of processing high counting rates, particularly by means of a DC-level controlled charge restoration for the preamplifier and a novel real-time correction of counting losses [3,4].

### 1.2 Neutron Energy and Neutron Flux Distribution

Several experimental and theoretical efforts have been made to determine the important neutron flux and neutron-energy distribution. The contribution of neutrons scattered in the structural material of the cylindrical target, the effects of scattering in the rabbit guide, rabbit and sample, and the influence of the neutron spectrum on the average activation cross section were considered in a thorough theoretical study [5,6]. Experimentally, the spectrum was investigated using two different techniques: a) the activity-ratio method by means of the (n,2n)-reactions on Zr and Nb as well as on Zr and U, and b) the reaction-threshold technique with 22 different element samples [7,8]. The Zr/U method yielded an average energy of 14.7 ± 0.1 MeV, whereas the other methods gave slightly lower values. A recent study [9] using the experimental results showed that the averaged neutron spectrum has a median at 14.7 MeV with a FWHM of 600 keV. The amount of thermal neutrons was determined by several (n,$\gamma$)-reactions to be less than $5 \times 10^{-3}$ of the total neutron flux.

The theoretically calculated neutron flux distribution was compared with activation measurements using small-sized wires at different positions inside the cylindrical target. The results confirm the rather constant neutron flux within the irradiation volume. The variation was determined to be within ± 5 % [10]. As a surprising result of this comparison it turned out that the divergence of the ion beam along the cylinder axis is much smaller than expected previously.

## 1.3 Reaction Cross-Section Measurements

The availability of the new high-intense 14 MeV neutron source has stimulated a considerable effort to measure unknown and to redetermine uncertain or well-known, but strongly energy-dependent cross-sections. Table I summarizes the results of the investigations [7,11,12,13,14] performed. The cross-section measurements have so far been concentrated on reactions with short-lived product nuclei, which are of particular interest in many applications, e.g. for activation-analysis work. In this connection (n,n')-reactions also come to the fore. Where comparable cross-section data are available, the agreement with other studies [see Ref. 11] is quite good. Deviations in the case of strongly energy-dependent reactions are not surprising.

Table I Cross Sections at 14.7 ± 0.3 MeV

| Reaction | σ (mb) | Ref. | Reaction | σ (mb) | Ref. |
|---|---|---|---|---|---|
| $^{50}$Ti(n,p)$^{50}$Sc | 14.3 ± 2.1 | [12] | $^{61}$Ni(n,p)$^{61}$Co<br>$^{62}$Ni(n,np)$^{61}$Co | 84 ± 4* | [13] |
| $^{50}$Cr(n,2n)$^{49}$Cr | 27.2 ± 1.9 | [13] | $^{62}$Ni(n,p)$^{62g}$Co | 24.8 ± 1.2 | [13] |
| $^{52}$Cr(n,p)$^{52}$V<br>$^{53}$Cr(n,np)$^{52}$V | 85.7 ± 2.6* | [13] | $^{62}$Ni(n,p)$^{62m}$Co | 14.6 ± 0.9 | [13] |
| $^{52}$Cr(n,2n)$^{51}$Cr<br>$^{50}$Cr(n,γ)$^{51}$Cr | 356 ± 24* | [13] | $^{64}$Ni(n,np)$^{63}$Co | 3.6 ± 0.7 | [13] |
| $^{53}$Cr(n,p)$^{53}$V | 47.2 ± 1.7 | [13] | $^{64}$Ni(n,α)$^{61}$Fe | 3.7 ± 0.2 | [13] |
| $^{54}$Cr(n,α)$^{51}$Ti<br>$^{53}$Cr(n,$^{3}$He)$^{51}$Ti | 12.6 ± 0.5* | [13] | $^{68}$Zn(n,p)$^{68g}$Cu | 5.0 ± 1.1 | [14] |
| $^{54}$Cr(n,p)$^{54}$V | 16.4 ± 0.5 | [13] | $^{68}$Zn(n,p)$^{68m}$Cu | 3.6 ± 0.6 | [14] |
| $^{55}$Mn(n,α)$^{52}$V | 23.2 ± 0.7 | [13] | $^{68}$Zn(n,α)$^{65}$Ni | 10.3 ± 1.8 | [14] |
| $^{55}$Mn(n,2n)$^{54}$Mn | 741 ± 22 | [13] | $^{79}$Br(n,n')$^{79m}$Br | 294 ± 16 | [ 7] |
| $^{54}$Fe(n,p)$^{54}$Mn | 307 ± 9 | [13] | $^{90}$Zr(n,p)$^{90m}$Y | 9.8 ± 1.7 | [14] |
| $^{54}$Fe(n,2n)$^{53}$Fe | 7.9 ± 0.7 | [13] | $^{90}$Zr(n,2n)$^{89m}$Zr | 75 ± 12 | [14] |
| $^{54}$Fe(n,α)$^{51}$Cr | 88 ± 6 | [13] | $^{90}$Zr(n,α)$^{87m}$Sr | 3.2 ± 0.5 | [14] |
| $^{56}$Fe(n,p)$^{56}$Mn<br>$^{57}$Fe(n,np)$^{56}$Mn | 111.0 ± 5.5* | [13] | $^{167}$Er(n,n')$^{167m}$Er | 252 ± 18 | [ 7] |
| $^{57}$Fe(n,p)$^{57}$Mn | 89 ± 5 | [13] | $^{168}$Er(n,2n)$^{167m}$Er | 581 ± 43 | [ 7] |
| $^{58}$Fe(n,p)$^{58}$Mn | 13.6 ± 0.7 | [13] | $^{168}$Er(n,2n)$^{167m}$Er<br>$^{167}$Er(n,n')$^{167m}$Er | 795 ± 59* | [ 7] |
| $^{59}$Co(n,p)$^{59}$Fe | 46.5 ± 2.3 | [13] | $^{174}$Yb(n,p)$^{174}$Tm | 3.0 ± 0.2 | [ 7] |
| $^{59}$Co(n,2n)$^{58}$Co | 231 ± 10 | [13] | $^{176}$Yb(n,n')$^{176m}$Yb | 19.7 ± 1.7 | [ 7] |
| $^{59}$Co(n,2n)$^{58m}$Co | 478 ± 24 | [13] | $^{183}$W(n,n')$^{183m}$W | 127 ± 14 | [ 7] |
| $^{59}$Co(n,α)$^{56}$Mn | 30.2 ± 1.5 | [13] | $^{184}$W(n,2n)$^{183m}$W | 656 ± 74 | [ 7] |
| $^{58}$Ni(n,p)$^{58g}$Co | 150.5 ± 6.0 | [13] | $^{184}$W(n,2n)$^{183m}$W<br>$^{183}$W(n,n')$^{183m}$W | 715 ± 81* | [ 7] |
| $^{58}$Ni(n,p)$^{58m}$Co | 169 ± 10 | [13] | $^{190}$Os(n,n')$^{190m}$Os | 14.0 ± 1.1 | [ 7] |
| $^{58}$Ni(n,np)$^{57}$Co | 586 ± 30 | [13] | $^{192}$Os(n,n')$^{192m}$Os | 2.6 ± 0.3 | [ 7] |
| $^{58}$Ni(n,2n)$^{57}$Ni | 34.7 ± 1.7 | [13] | $^{191}$Ir(n,n')$^{191m}$Ir | 221 ± 22 | [ 7] |
| $^{60}$Ni(n,p)$^{60}$Co | 131 ± 4** | [13] | $^{208}$Pb(n,2n)$^{207m}$Pb<br>$^{207}$Pb(n,n')$^{207m}$Pb | 1365 ± 68* | [ 7] |

* The value is calculated taking the abundance of the first mentioned isotope.

** The value refers to the sum of groundstate and isomeric state cross-sections.

References

[ 1 ] H.-U. Fanger, R. Pepelnik, W. Michaelis
J. Radioanal. Chem. 61 (1981) 147

[ 2 ] K.A. Schmidt, H. Dohrmann
Atomkernenergie 27 (1976) 159

[ 3 ] G.P. Westphal
J. Radioanal. Chem. 70 (1982) 387

[ 4 ] R. Pepelnik, G.P. Westphal, B. Anders
Nucl. Instr. and Meth., to be published

[ 5 ] B.M. Bahal, H.-U. Fanger
GKSS 82/E/22

[ 6 ] B.M. Bahal, H.-U. Fanger
Nucl. Instr. and Meth. 211 (1983) 469

[ 7 ] B. Anders, R. Pepelnik, H.-U. Fanger
Proceedings of the International Conference, Antwerp, 6 - 10 Sept. 1982
K.H. Böckhoff (Ed.): Nuclear Data for Science and Technology, p. 859

[ 8 ] B. Anders
Interner Zyklotronbericht HH 83-01, Universität Hamburg

[ 9 ] B.M. Bahal, H.-U. Fanger
Nucl. Instr. and Meth. 220A (1984) 517

[10] B. Anders, E. Bössow
GKSS 83/E/23

[11] W. Michaelis
IAEA Consultants' Meeting on Nuclear Data Techniques, Krakow, Poland
14 - 18 Nov. 1983

[12] J.L. Barreira Filho, H.-U. Fanger
GKSS 81/E/53

[13] B.M. Bahal, R. Pepelnik
GKSS, to be published

[14] J.L. Barreira Filho, H.-U. Fanger
GKSS 82/E/8

INSTITUT FÜR KERNCHEMIE
UNIVERSITÄT ZU KÖLN

## 1. Measurement and Hybrid Model Analysis of Integral Excitation Functions for p-induced Reactions up to 200 MeV

R. Michel, F. Peiffer, R. Stück

### 1.1 Proton-induced Reactions on V, Mn and Co

By irradiation experiments at the "Cyclon" isochronous cyclotron at Louvain La Neuve and the synchrocyclotron of the IPN Orsay we extended our earlier measurements of integral excitation functions [1,2] from 45 MeV to 200 MeV [cf.3].

The cross sections were determined using the stacked foil technique. Three types of stacks covered the energy ranges from 45 to 80 MeV, from 77 to 160 MeV and from 150 to 200 MeV. The p-fluxes were determined by the $^{22}$Na activity induced in Al-foils distributed all over the stacks. As monitor cross sections for the reaction $^{27}$Al(p,3p3n)$^{22}$Na the "valeur adopte" of Tobailem and de Lassus St. Genies [4] were taken. The nuclear data used for the calculation of cross sections were the same as in [1,2 and 3]. Since the energy ranges of the different experiments are overlapping, also with our earlier measurements below 45 MeV [1], the quality of the absolute determination of the cross sections was checked with high sensitivity with regard to flux determination errors. Moreover the negligibility of secondary particles was proved by applying the method to reactions with low threshold energies.

So we now have a comprehensive, self-consistent set of excitation functions up to 200 MeV.
These new cross sections allow for a much more detailed analysis with regard to nuclear reaction theories. By a coincidence an improved version of the computer code "ALICE LIVERMORE 82" [5] was at our disposal (courtesy of M. Blann), which now includes the Wapstra and Gove mass tables [6] and which, moreover, in contrast to the earlier version of the

hybrid model of preequilibrium reactions [7,8] now includes multiple preequilibrium emission. Further it allows to take into account broken exciton numbers according to [9].

According to M. Blann [10] this version should be capable to perform <u>a priori</u> calculations up to 200 MeV. Since the target elements Mn and Co are, and V can be regarded, as single isotope elements, the comparsion of theoretical and experimental cross sections is of particular interest here. It turns out that, for some reactions and generally for higher energies, severe discrepancies are to be observed in <u>a priori</u> calculations. Therefore a set of optimal parameters was searched for. But this search did not result in an unambiguous choice of parameters [11]. While generally (p,xn)-reactions are fairly well represented by the theory [1,12],

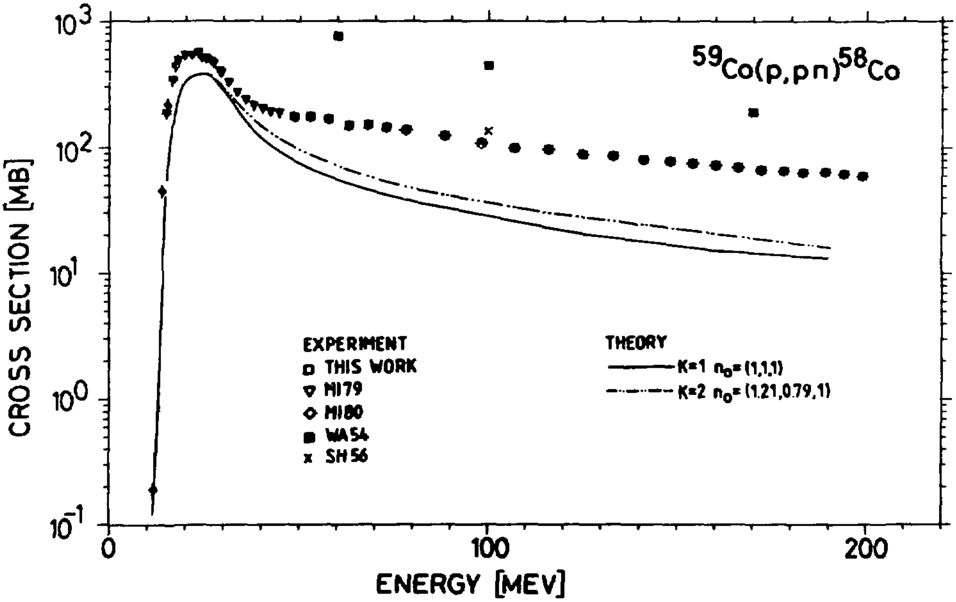


Fig. 1 Experimental cross sections and theoretical excitation functions for the reaction $^{59}Co(p,pxn)\ ^{58}Co$. For references of other authors see [3], for the work of other authors below 45 MeV see [1].

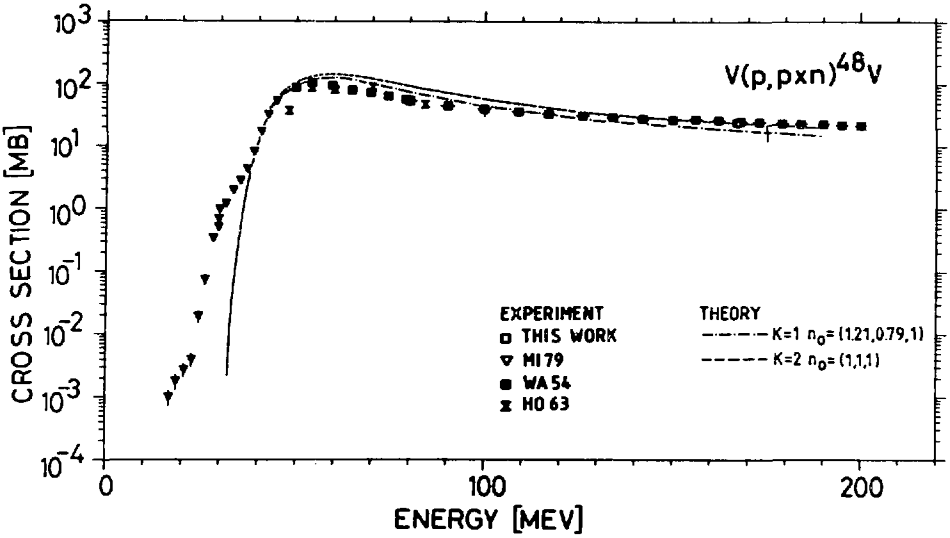


Fig.2 Experimental cross sections and theoretical excitation functions for the reaction $V(p,pxn)^{48}V$. For references of other authors see [3], for the work of other authors below 45 MeV see [1].

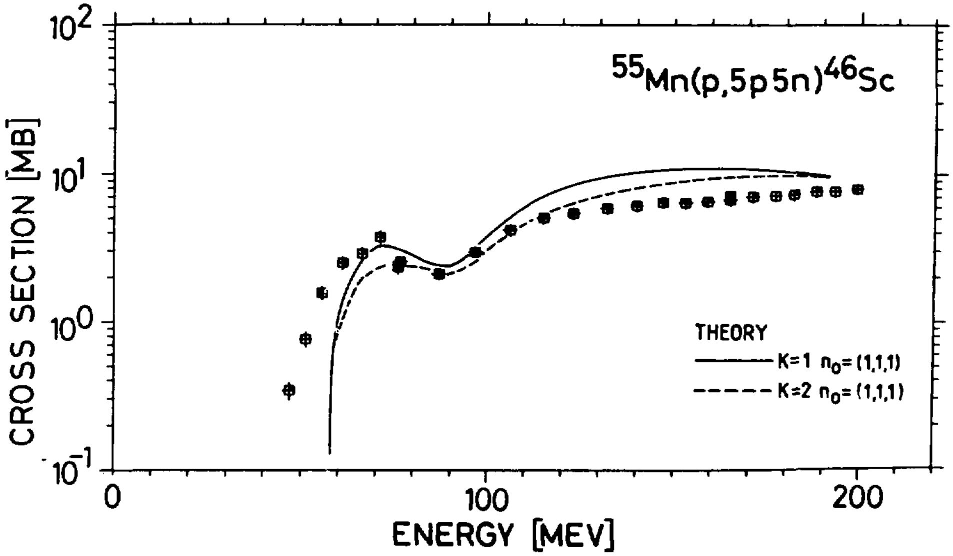


Fig.3 Experimental cross sections and theoretical excitation functions for the reaction $^{55}Mn(p,5p5n)^{46}Sc$.

for (p,pn)-reactions strong discrepancies between theory and experiment were seen, pointing to important contributions of direct reactions at high energies (fig.1). These discrepancies vanish, however, for (p,pxn)- reactions with increasing x (fig.2) and also for some reactions with higher threshold energies (fig.3). Generally, the observed discrepancies are not so extreme as observed for α- and $^{3}$He-induced reactions [13,14]. The capability of *a priori* calculations is, however, relatively limited, since there exist still too many reactions exhibiting severe discrepancies which have to be studied in more detail [11].

### 1.2 Proton-induced Reactions on Ti, Fe and Ni between 45 and 80 MeV

For the cosmochemically important target elements Ti, Fe and Ni the gap between our earlier measurements below 45 MeV [1,15,16] and those above 80 MeV [18] was closed in the experiments at Louvain La Neuve. Tables 1-3 give these results for these target elements. The data fit extremely well with those of the earlier determination and do not change any statement of our earlier discussion of these excitation functions with regard to the theories of nuclear reactions [17]. The determination of excitation functions relevant to cosmochemistry is now continued by measurements at 600 MeV.

Table I Cross sections (mb) of proton induced reactions on natural titanium between 50 and 80 MeV

| $E_p$[MeV] | $^{48}$Sc | $^{47}$Sc | $^{46m+g}$Sc | $^{44m}$Sc | $^{47}$Ca | $^{43}$K | $^{42}$K |
|---|---|---|---|---|---|---|---|
| 79.47 ± 0.34 | 1.92 ±0.17 | 22.7 ± 3.0 | 49.5 ± 6.9 | 23.0 ± 2.3 | 0.052 ±0.012 | 1.34 ±0.19 | 5.7 ±1.0 |
| 74.93 ± 0.44 | 1.94 ±0.19 | 21.3 ± 2.8 | 47.0 ± 6.6 | 21.9 ± 2.0 | 0.050 ±0.012 | 1.22 ±0.17 | 5.6 ±0.9 |
| 70.27 ± 0.51 | 2.08 ±0.21 | 22.8 ± 3.0 | 50.4 ± 7.1 | 22.7 ± 2.3 | 0.057 ±0.012 | 1.25 ±0.19 | 6.2 ±1.2 |
| 65.26 ± 0.57 | 2.10 ±0.23 | 22.5 ± 2.9 | 51.2 ± 7.1 | 20.4 ± 1.8 | 0.044 ±0.010 | 1.20 ±0.16 | 6.0 ±1.0 |
| 60.09 ± 0.63 | 2.19 ±0.22 | 23.7 ± 3.1 | 55.2 ± 7.7 | 17.4 ± 1.7 | 0.048 ±0.014 | 1.32 ±0.20 | 5.29 ±0.85 |
| 54.43 ± 0.68 | 2.22 ±0.20 | 24.0 ± 3.1 | 59.9 ± 7.8 | 14.9 ± 1.5 | 0.041 ±0.012 | 1.44 ±0.19 | 3.51 ±0.56 |
| 50.32 ± 0.72 | 2.01 ±0.18 | 21.5 ± 2.8 | 59.5 ± 7.7 | 12.4 ± 1.1 | | 1.26 ±0.16 | 1.43 ±0.29 |

Table II Cross sections (mb) of p-induced reactions on natural iron between 79 and 49 MeV

| $E_p$ [MeV] | $^{54}Mn$ | $^{52}Mn$ | $^{51}Cr$ | $^{48}Cr$ | $^{48}V$ | $^{47}Sc$ | $^{46m+g}Sc$ | $^{44m}Sc$ |
|---|---|---|---|---|---|---|---|---|
| 78.25 ± 0.39 | 77.3 ± 6.2 | 32.5 ± 2.9 | 65.5 ± 5.2 | 0.319 ±0.048 | 6.16 ±0.60 | 0.249 ±0.045 | 1.00 ±0.12 | 0.239 ±0.033 |
| 73.66 ± 0.49 | 83.0 ± 6.6 | 34.5 ± 3.1 | 59.3 ± 4.7 | 0.278 ±0.042 | 4.62 ±0.41 | 0.240 ±0.043 | 0.621 ±0.087 | 0.228 ±0.032 |
| 68.94 ± 0.56 | 85.3 ± 6.8 | 33.2 ± 3.0 | 52.5 ± 4.2 | 0.289 ±0.049 | 4.00 ±0.37 | 0.222 ±0.038 | 0.231 ±0.028 | 0.179 ±0.034 |
| 63.85 ± 0.63 | 88.6 ± 7.1 | 27.4 ± 2.5 | 51.9 ± 4.2 | 0.295 ±0.050 | 4.28 ±0.39 | 0.152 ±0.026 | 0.051 ±0.011 | 0.089 ±0.020 |
| 58.59 ± 0.68 | 98.1 ± 7.8 | 19.8 ± 1.8 | 60.7 ± 4.9 | 0.251 ±0.043 | 5.10 ±0.45 | 0.063 ±0.014 | | |
| 53.46 ± 0.74 | 114.8 ± 9.2 | 14.9 ± 1.5 | 76.6 ± 6.1 | 0.160 ±0.030 | 5.64 ±0.48 | 0.031 ±0.007 | | |
| 49.30 ± 0.78 | 122.8 ± 9.8 | 12.2 ± 1.1 | 86.3 ± 6.9 | 0.053 ±0.017 | 4.71 ±0.39 | | | |

Table III Cross sections (mb) of p-induced reactions on natural nickel between 78 and 48 MeV

| $E_p$ [MeV] | $^{57}Ni$ | $^{58m+g}Co$ | $^{57}Co$ | $^{56}Co$ | $^{55}Co$ | $^{54}Mn$ | $^{52}Mn$ | $^{51}Cr$ | $^{48}V$ | $^{46m+g}Sc$ |
|---|---|---|---|---|---|---|---|---|---|---|
| 77.53 ± 0.43 | 2.61 ±0.29 | | | 37.9 ± 4.9 | 5.69 ±0.74 | 36.5 ± 4.3 | 13.2 ± 1.2 | 16.6 ± 1.3 | 0.44 ±0.16 | 0.139 ±0.026 |
| 72.89 ± 0.55 | 2.80 ±0.34 | 145 ± 13 | 111 ± 17 | 38.7 ± 3.8 | 6.28 ±0.82 | 30.2 ± 2.7 | 14.2 ± 1.3 | 10.03 ± 0.90 | 0.147 ±0.047 | 0.076 ±0.017 |
| 68.13 ± 0.62 | 3.06 ±0.34 | 151 ± 14 | 114 ± 18 | 43.0 ± 4.7 | 6.63 ±0.86 | 25.9 ± 2.3 | 12.9 ± 1.2 | 5.06 ± 0.56 | 0.027 ±0.010 | |
| 63.01 ± 0.67 | 3.18 ±0.38 | 149 ± 14 | 110 ± 18 | 46.9 ± 4.7 | 5.44 ±0.71 | 22.4 ± 2.0 | 8.01 ± 0.72 | 3.29 ± 0.40 | | |
| 57.70 ± 0.73 | 3.94 ±0.39 | 168 ± 15 | 126 ± 18 | 60.0 ± 6.0 | 3.98 ±0.52 | 26.8 ± 2.1 | 3.94 ± 0.35 | 4.67 ± 0.51 | | |
| 52.81 ± 0.81 | 4.77 ±0.48 | 176 ± 16 | 142 ± 20 | 69.4 ± 6.3 | 2.15 ±0.30 | 33.0 ± 2.6 | 1.83 ± 0.20 | 6.23 ± 0.68 | | |
| 48.61 ± 0.84 | 5.87 ±0.59 | 175 ± 16 | 154 ± 22 | 63.5 ± 6.4 | 0.87 ±0.19 | 40.0 ± 3.6 | 0.66 ± 0.14 | 6.94 ± 0.76 | | |

References

[1] R. Michel, G. Brinkmann, H. Weigel and W. Herr, Nucl.Phys. A 322 (1972) 40

[2] R. Michel, G. Brinkmann and W. Herr, NEA-NDC (E)-202 U Vol.V INDC(GER) -21/L + Special (1979) 78

[3] R. Stück, Thesis (1983), Universität zu Köln

[4] Tobailem and de Lassus St. Genies, CEA-N-1466(3) (1975)

[5] M. Blann, LLNL-Report (1982) UCID-19614

[6] A.H. Wapstra and N.B. Gove, Nuklear Data Tables 9 (1971) 265

[7] M. Blann, Phys.Rev.Lett. 27 (1971) 337

[8] M. Blann, COO-3494-10 (1973), COO-3494-29 (1976)

[9] M. Blann, H.K. Vonach, UCRL-Preprint-88540 Dec.82

[10] M. Blann, priv.comm. (1983)

[11] R. Michel, F. Peiffer and R. Stück, to be published 1984

[12] R. Michel, G. Brinkmann, J.Radioanal.Chem. 59 (1980) 467

[13] R. Michel and G. Brinkmann, Nucl.Phys. A338 (1980) 167

[14] R. Michel and M. Galas, Nucl.Phys. A404 (1983) 77

[15] R. Michel, G. Brinkmann, H. Weigel and W. Herr, J.Inorg.Nucl.Chem. 40 (1978) 1845

[16] R. Michel, H. Weigel and W. Herr, Z.Phys. A286 (1978) 393

[17] R. Michel and R. Stück, Proc. 14th Lun. Plan. Sci. Conf. J.Geophys.Res. 89 (1984) B673

INSTITUT FÜR KERNCHEMIE

JOHANNES GUTENBERG UNIVERSITÄT MAINZ

## Nuclear Charge Distribution of Heavy Mass Fission Products in $^{235}U(n_{th}, f)$

H.O. Denschlag, Z.B. Alfassi*, H. Braun, W. Ditz, W. Faubel, H. Faust**, St. Hörner, W. Pörsch, R. Sehr, H. Schrader**, and B. Sohnius

Fission products were separated according to mass, ionic charge state, and kinetic energy using the mass separator LOHENGRIN of the Institut Laue-Langevin (Grenoble). The yields of the single members within mass chains 130 to 147 were obtained by measuring the gamma rays emitted from the short-lived fission products immediately following their beta-decay. Absolute gamma-ray line intensities and branching ratios - when not known - were determined by separate radiochemical experiments [1,2,3].

The mass separator LOHENGRIN provides fission products of a well defined kinetic energy and of the ionic charge state realized while in transit through the separator. This feature is advantageous for a fundamental investigation of e.g. the correlation between specific scission configurations and fission yields and for the study of the

---------------

* Ben Gurion University of the Negev, Beer Sheva, Israel

** Institut Laue-Langevin, Grenoble, France

dynamical ionization behaviour of heavy ions and related effects. For practical purposes and for a comparison with radiochemical yields, in principle, the yields at the various kinetic energies of the fragments and their various ionic charge states ought to be averaged. Such an analysis will be attempted in the future.

At present, in Table I we are presenting yields obtained for the mean kinetic energy and for the mean ionic charge state. These yields can be expected to generally agree with the averaged values except for chain 142 where the fission yields observed vary in a particularly strong way with the ionic charge state chosen. In this case, a summation over the charge states has been performed and the following yield values (relative to a "fractional cumulative yield" (YFC) of $^{142}Ba$ of 100%) have been obtained:

$$YFC\ (^{142}Cs) = (37 +/- 4)\ \%$$

$$YFI\ (^{142}Ba) = (63 +/- 7)\ \%$$

These yields and the yields within the other mass chains (130 to 137 and 139 to 147)* given in Table I are in general agreement with the radiochemical yield values [4].

The total results including values obtained at other kinetic energies of the fragments and at other ionic charge states for the respective mass chains may be found in the references given in the table for the respective mass chains.

---------------

* Mass chain 138 [6] has not been finally evaluated yet.

Table I Fractional independent (first chain members: -cumulative) yields in $^{235}U(n_{th}, f)$ measured at the mean kinetic energy of the fission fragments and at the mean ionic charge state of the fragments in transit through LOHENGRIN

| Nuclide | Fractional Yield | References |
|---|---|---|
| $^{130}Sn$ | 0.69 +/- 0.04 | [6] |
| $^{130}Sb$ | 0.28 +/- 0.04 | [6] |
| $^{130}Te$ | 0.03 +/- 0.09 | [6] |
| $^{131}Sn$ | 0.34 +/- 0.02 | [6] |
| $^{131}Sb$ | 0.62 +/- 0.02 | [6] |
| $^{131}Te$ | 0.04 +/- 0.02 | [6] |
| $^{132}Sn$ | 0.14 +/- 0.02 | [5] |
| $^{132}Sb$ | 0.45 +/- 0.03 | [5] |
| $^{132}Te$ | 0.41 +/- 0.03 | [5] |
| $^{133}Sb$ | 0.44 +/- 0.02 | [5, 7] |
| $^{133}Te$ | 0.56 +/- 0.02 | [5, 7] |
| $^{134}Sb$ | 0.06 +/- 0.01 | [5, 8] |
| $^{134}Te$ | 0.82 +/- 0.08 | [5, 8] |
| $^{134}I$ | 0.12 +/- 0.02 | [5, 8] |
| $^{135}Sb$ | 0.06 +/- 0.03 | [5, 7] |
| $^{135}Te$ | 0.50 +/- 0.03 | [5, 7] |
| $^{135}I$ | 0.42 +/- 0.02 | [5, 7] |
| $^{135}Xe$ | 0.02 +/- 0.01 | [5, 7] |
| $^{136}Te$ | 0.16 +/- 0.04 | [5, 8] |
| $^{136}I$ | 0.42 +/- 0.08 | [5, 8] |
| $^{136}Xe$ | 0.42 +/- 0.15 | [5, 8] |
| $^{137}Te$ | 0.08 +/- 0.01 | [5] |
| $^{137}I$ | 0.43 +/- 0.05 | [5] |
| $^{137}Xe$ | 0.49 +/- 0.05 | [5] |
| $^{139}I$ | 0.19 +/- 0.03 | [7] |
| $^{139}Xe$ | 0.74 +/- 0.04 | [7] |
| $^{139}Cs$ | 0.08 +/- 0.05 | [7] |
| $^{139}Ba$ | 0.02 +/- 0.05 | [7] |
| $^{140}I$ | 0.04 +/- 0.02 | [6] |
| $^{140}Xe$ | 0.72 +/- 0.02 | [6] |
| $^{140}Cs$ | 0.22 +/- 0.02 | [6] |
| $^{140}Ba$ | 0.03 +/- 0.05 | [6] |

Table I (continued)

| Nuclide | Fractional Yield | References |
|---|---|---|
| $^{141}Xe$ | 0.16 +/- 0.01 | [6] |
| $^{141}Cs$ | 0.47 +/- 0.03 | [6] |
| $^{141}Ba$ | 0.37 +/- 0.02 | [6] |
| $^{142}Cs$ | 0.22 +/- 0.01* | [9] |
| $^{142}Ba$ | 0.78 +/- 0.01* | [9] |
| $^{143}Cs$ | 0.25 +/- 0.04 | [9] |
| $^{143}Ba$ | 0.67 +/- 0.05 | [9] |
| $^{143}La$ | 0.08 +/- 0.07 | [9] |
| $^{144}Cs$ | 0.02 +/- 0.01 | [9] |
| $^{144}Ba$ | 0.77 +/- 0.04 | [9] |
| $^{144}La$ | 0.21 +/- 0.04 | [9] |
| $^{145}Ba$ | 0.45 +/- 0.03 | [9] |
| $^{145}La$ | 0.55 +/- 0.04 | [9] |
| $^{145}Ce$ | < 0.024 | [9] |
| $^{146}Ba$ | 0.28 +/- 0.03 | [9] |
| $^{146}La$ | 0.52 +/- 0.08 | [9] |
| $^{146}Ce$ | 0.20 +/- 0.01 | [9] |
| $^{146}Pr$ | < 0.012 | [9] |
| $^{147}La$ | 0.41 +/- 0.01 | [9] |
| $^{147}Ce$ | 0.41 +/- 0.08 | [9] |
| $^{147}Pr$ | 0.18 +/- 0.08 | [9] |

*Yield not directly comparable to radiochemical yield (see text)

References

[1] H. Braun, T. Izak-Biran, Z. Alfassi, W. Lauppe, H.O Denschlag in: Progress Report on Nuclear Data Research in the Federal Republic of Germany (1979), Report NEANDC(E)-202 U Vol V and INDC(Ger)-21/L+Special, p. 74

[2] B. Sohnius, M. Brügger, H.O. Denschlag in: Progress Report on Nuclear Data Research in the Federal Republic of Germany (1982), Report NEANDC(E)-232 U Vol V and INDC(Ger)-24/L+Special, p. 46

[3] B. Sohnius, B. Pfeiffer, H.O. Denschlag in: Progress Report on Nuclear Data Research in the Federal Republic of Germany (1983), Report NEANDC(E)-242 U Vol V and INDC(Ger)-26/L+Special, p. 47

[4] B.F. Rider, M.E. Meek, Report NEDO-12154-2(D) (1977)

[5] H.O. Denschlag, H. Braun, W. Faubel, G. Fischbach, H. Meixler, G. Paffrath, W. Pörsch, M. Weis, H. Schrader, G. Siegert, J. Blachot, Z.B. Alfassi, H.N. Erten, T. Izak-Biran, T. Tamai, A.C. Wahl, and K. Wolfsberg, in Physics and Chemistry of Fission (Proceedings Symp. Jülich, 1979), IAEA, Vienna (1980), Vol. II, p. 153

[6] W. Pörsch, Dissertation, Mainz, in preparation

[7] H. Braun, Dissertation, Mainz (1983)

[8] W. Faubel, Dissertation, Mainz, (1980)

[9] B. Sohnius, Dissertation, Mainz, in preparation.

INSTITUT FÜR STRAHLENPHYSIK
UNIVERSITÄT STUTTGART

## Investigations of Analyzing Power and Differential Cross Section of Lead-2o8, Lead-2o6, Thorium-232, Tantalum, Tungsten and Thulium for $E_n$ = 7.75 MeV

G. Bulski, W. Grum, J.W. Hammer, K.-W. Hoffmann,
G. Schleußner+, G. Schreder

Studies with the Stuttgart facility SCORPION for fast polarized neutron scattering experiments for the measuring of analyzing power and differential cross section for heavy mass and medium mass nuclei have been continued. At an energy of 7.75 MeV for the polarized neutrons of 6o % polarization investigations on $^{208}Pb$, $^{206}Pb$, $^{232}Th$, Ta, W and Tm have been performed. The accuracy of the data and also of the data analysis could be improved. For $^{208}Pb$ and Tm only very small samples were available, therefore we had to measure near the sensitivity limit of our set up.

---

+ Deceased 1983

Fig. 1 and 2 give examples of the data for $^{206}Pb^{*}$.

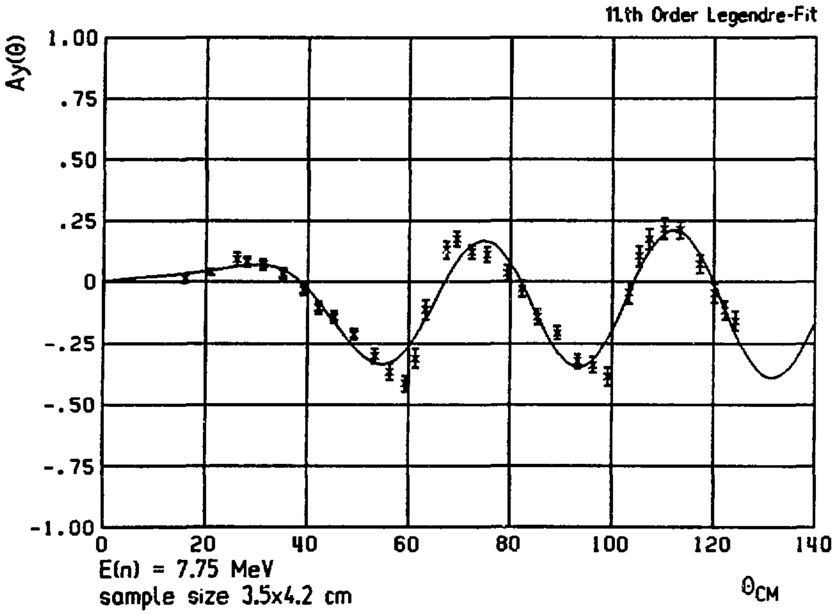


Fig. 1 Analyzing Power of Lead-206 for $E_n$ = 7.75 MeV

The analysis of the data, like finite sample corrections and optical model calculations is in progress. Finite sample corrections for the analyzing power evaluations are made using the code JANE by E. Woye. This code will be adapted to correct also differential cross section data.

---

* The lending of a $^{206}Pb$ sample by J. Harvey, Oak Ridge, is highly appreciated. Also we were in debt of gratitude to G. Haouat, Bruyères le Châtel, for lending us the $^{208}Pb$ sample.

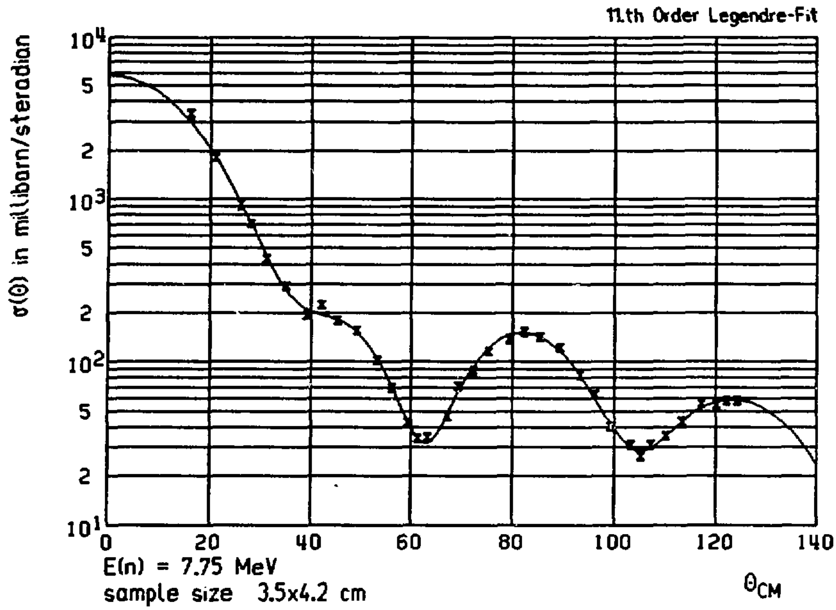


Fig. 2 Differential cross section of Lead-206 for $E_n$ = 7.75 MeV

The code FANTI for the unfolding of proton recoil data, based on the older codes FERDOR and FORIST, has been proven in many cases, even worse ones, and is now completed. It will be available on request.

REAKTORSTATION GARCHING; FACHBEREICH PHYSIK
TECHNISCHE UNIVERSITÄT MÜNCHEN

## Coherent Neutron Scattering Lengths and Free Scattering Cross Sections

1. Gallium and Zinc

   L. Koester, K. Knopf, W. Waschkowski

Bound coherent neutron scattering lengths b and free cross sections $\sigma_s$ were measured on natural Ga and Zn and on isotopically enriched samples. We obtained by means of Christiansen filter technique and transmission measurements the following data (to be published):

| | |
|---|---|
| $b(^{nat}Ga)$ = 7.288 (15) fm, | $\sigma_{s/1.26\ eV}$ = 6.994 (11) b, |
| | $\sigma_{s/5.19\ eV}$ = 6.899 (7) b, |
| | $\sigma_{s/18.8\ eV}$ = 6.773 (14) b, |
| $b(^{69}Ga)$ = 7.91 (4) fm, | $\sigma_{s/1.26\ eV}$ = 8.23 (6) b, |
| | $\sigma_{s/5.2\ eV}$ = 8.49 (16) b, |
| $b(^{71}Ga)$ = 6.36 (3) fm. | |

From the energy dependence of the scatting cross section of Ga additional data on the resonance parameters could be derived.

| | |
|---|---|
| $b(^{nat}Zn)$ = 5.686 (14) fm, | $\sigma_{s/1.26\ eV}$ = 4.040 (6) b, |
| $b(^{64}Zn)$ = 5.23 (2) fm, | $\sigma_{s/1.26\ eV}$ = 3.54 (10) b, |
| $b(^{66}Zn)$ = 5.98 (3) fm, | $\sigma_{s/1.26\ eV}$ = 4.32 (12) b, |
| $b(^{67}Zn)$ = 7.58 (4) fm, | |
| $b(^{68}Zn)$ = 6.04 (2) fm. | |

2. Thorium

L. Koester, K. Knopf, W. Waschkowski

In continuation of our measurements of coherent bound scattering lengths and free scattering cross sections we obtainded the following nuc`ear data for thorium (to be published):

b = 10.30 (4) fm, $\sigma_{s/1.26\ eV}$ = 12.84 (16) b,

$\sigma_{s/5.2\ eV}$ = 12.42 (18) b,

$\sigma_{s/144\ keV}$ = 12.70 (10) b.

These values are in good agreement with the resonance parameters if we accept a bound level at -5.1 eV with the width of $g\Gamma_n^o$ = 2.07 meV [1] .

3. Tellurium and Antimony

L. Koester, K. Knopf, W. Waschkowski

By means of Christiansen filter technique and transmission measurements we obtained the following coherent scatting lengths and total cross sections on natural tellurium and natural antimony:

b (Te) = 5.786 (14) fm, $\sigma_{tot/1.26\ eV}$ = 6.68 (2) b,

$\sigma_{tot/5.2\ eV}$ = 4.65 (2) b,

b (Sb) = 5.54 (3) fm, $\sigma_{tot/1.26\ eV}$ = 4.09 (2) b,

$\sigma_{tot/5.2\ eV}$ = 9.17 (5) b.

Reference:

[1] G. Vasiliu, S. Mateescu, D. Gheorghe, M. Diodaru, E. Badescu, N. Dragon, O. Bujoreanu, C. Cracium, L. Pintiliescu, M. Zaharcu, D. Popescu, P. Statnicov, V. Arrigeanu: INDC (RUM) - 10 (1980)

INSTITUT FÜR KERNCHEMIE

PHILIPPS-UNIVERSITÄT MARBURG

## 1. Gamma-Ray Catalog

U. Reus, W. Westmeier

Quantitative information on gamma rays from the decay of radioactive nuclides is required in many areas of nuclear science as well as related fields. We have therefore produced a compilation of decay properties of all known radionuclides, with the main emphasis on energies and absolute intensities of gamma rays. A first printed version of this catalog was issued in 1979, covering references to the literature through June 1978.

Revision of data for a second edition, including references through June 1982, was completed in 1983. The updated version contains information on 2526 nuclides and isomers with a total of more than 47,000 gamma rays and X-rays, the information on X-rays accompanying radioactive decay being a newly introduced feature. As before, the catalog is presented in two parts: In Part I gamma rays are listed in order of increasing energy for the purpose of identification of unknown gamma lines. In Part II complete data sets for each nuclide are listed in order of mass number A and nuclear charge Z of the nuclides. This part also contains additional information, references, and comments in case of any discrepancies.

The revised catalog has been published in "Atomic Data and Nuclear Data Tables", Volume 29, 1-406 (1983).

## 2. Alpha-Energy Table

W. Westmeier, R.A. Esterlund

A table of alpha-decay properties of all known alpha-emitting nuclides, which includes data on alpha energies, intensities, and the abundance of the alpha branch, is being compiled. The table is ordered by increasing energy and covers data on 534 alpha emitters with a total of 1621 energies at present.
Computer printout copies of the table are available on request.

PHYSIKALISCH-TECHNISCHE BUNDESANSTALT
BRAUNSCHWEIG

## 1. Neutrons from $^{9}Be + d$

H. J. Brede, G. Dietze, K. Kudo*

The reaction $^{9}Be + d$ is used as an intense neutron source at the facility for the calibration of neutron therapy dosimeters. The purpose of these investigations is an accurate determination of the spectral neutron yield from the target which can be used to calculate the tissue kerma in free air at the reference position of the neutron field ("fluence method").

The neutron yield and the neutron spectrum, emitted from an air-cooled 2 mm thick Be target which was bombarded by deuterons from the PTB cyclotron were measured with various deuteron energies from 9.4 MeV to 13.3 MeV. The time-of-flight spectrometer with a flight path of 12 m [1] and an NE 213 scintillation detector (5.07 cm in height, 5.06 cm in diameter) was used. The pulsed beam of the cyclotron and conventional n-$\gamma$ discrimination techniques were applied. The detector efficiency was determined for various bias values using the Monte Carlo code NEFF4 [2].

The neutron spectra were measured in the neutron energy range from 0.4 MeV to 17 MeV. The neutron yield at 0° to the direction of the incident deuterons was obtained for deuteron energies from 9.4 MeV to 13.3 MeV. At $E_d$ = 12.4 MeV and 13.3 MeV the neutron yields for angles of emission up to 40° were determined. At a distance of 80 cm from the target, the neutron fluence and the tissue kerma in air in relation to the deuteron energy were also evaluated.

In addition to this, the influence of a small water-cooling system at the target backing and the influence of the collimator system on the neutron yield and on the spectral fluence were investigated.

*Electrotechnical Laboratory, Ibaraki, Japan

## 2. Angular Distribution of the Reaction $D(d,n)^3He$ for $3.0 \leq E_d \leq 11$ MeV

H. Klein, R. Böttger , J. Suita*

Discrepancies in the calibration of the neutron detection efficiency of liquid scintillators [1] gave rise to an investigation of the D(d,n) reaction for deuteron energies from 3.0 MeV up to 11.0 MeV in steps of 0.5 MeV.

In the energy range 6.3 MeV $\leq E_n \leq$ 14 MeV a liquid scintillator NE 213 (10.6 cm in diameter and 2.54 cm in length), was carefully calibrated in steps of 0.5 MeV with reference to a proton recoil telescope. The experimentally determined response spectra could be reproduced in absolute scale to within a standard deviation of ± 2 % by the Monte Carlo code NRESP4 [2].

On the basis of this calibration the angular distribution of the neutrons from the reaction $D(d,n)^3He$ were measured for emission angles $0 \leq \vartheta_n^{LAB} \leq 90°$. The experimental yield will be compared with the expected yield as calculated by means of the MC code SINENA [3] on the basis of recently evaluated cross sections [4].

Preliminary results showed significant deviations up to 15 % increasing with the projectile energy and the emission angle. The final analysis is in progress.

---

*IAEA fellow from IEN, Rio de Janeiro

## 3. Neutrons in the Energy Range $E_n$ = 0.5 - 30 keV from the Reaction $^{45}Sc(p,n)^{45}Ti$

M. Cosack, H. Lesiecki, J.B. Hunt*

For the testing of radiation protection instruments with neutrons in the energy range from about 0.5 to 50 keV only a few neutron sources are available. The $^{45}Sc(p,n)^{45}$ reaction seems to be very useful for this purpose, as by bombarding a scandium target with protons with energies of a few keV above the threshold of 290.8 keV, low energetic neutrons can be produced. In order to investigate the structure of the neutron yield a thick Sc-target was bombarded with a pulsed proton beam and the neutron energies were analyzed by means of time-of-flight technique with a lithium glass scintillator. At the emission angle of 0° strong resonances at 8.2; 14.5; 16.8; 27.5; 33.6 and 36.7 keV were found with only a small neutron yield in between. The natural line width of these resonances was in most cases less than 0.5 keV. Due to the kinematics of the reaction, the energy of each resonance decreases when the emission angle increases. The yields and energies of the most prominent resonances were investigated for different emission angles. Especially the resonance of 8.2 keV at 0° emission produces neutrons of about 0.5 keV at 120° emission. The $^{45}Sc(p,n)$ was also used to produce monoenergetic neutrons, taking a thin Sc-target and bombarding it with protons whose energy was adjusted in order to produce neutrons of one of the resonances. For the 8.2 keV resonance and a proton beam of 100 µA on a thin target a neutron flux density of $2 \cdot 10^5$ $sr^{-1}$ $s^{-1}$ was determined with a De Panger long counter. For the 27.5 keV resonance the flux density was $1.8 \cdot 10^5$ $sr^{-1}$ $s^{-1}$. These flux densities were found to be sufficient to calibrate radiation protection survey meters.

---

*NPL, Teddington, G.B.

## References

[1] R. Böttger, H.J. Brede, M. Cosack, G. Dietze, R. Jahr, H. Klein, H. Schölermann and B.R.L. Siebert
Proc. of the Int. Conf. on Nuclear Data for Science and Technology, Antwerp, 1982, ed. K.H. Böckhoff, Reidel Publ. Comp. Dordrecht (1983) p. 836

[2] G. Dietze and H. Klein
PTB-report ND-22, Braunschweig, Oct. 1982

[3] B.R.L. Siebert, H.J. Brede and H. Lesiecki
PTB-report ND-23, Braunschweig, Nov. 1982

[4] M. Drosg
Nucl. Sci. Eng. 67 (1978) 19o

FACHINFORMATIONSZENTRUM ENERGIE PHYSIK MATHEMATIK

Status Report

H. Behrens, G. Ebel, H.W. Müller

## 1. Cooperation between the Fachinformationszentrum and Chemical Abstracts Service

The American Chemical Abstracts Service (CAS) and the Fachinformationszentrum are joining their online computer services. The computers of CAS in Columbus and of FIZ at Karlsruhe will be linked and the same computer software will be used in both facilities. The new network established is named "STN International". The bibliographic and numerical data bases implemented at both locations can be accessed by the user via both nodes of the network.

## 2. New Data compilations

The following new issues in the series Physics Data were published during the period of this report:

| | |
|---|---|
| 4-3 (1983) | Compilation of Coupling Constants and Low-Energy Parameters. 1983 Edition.<br>U. Dumbrajs, R. Koch, H. Pilkuhn, G.C. Oades, H. Behrens, J.J. de Swart, P. Kroll |
| 5-22 (1983) | Gases and Carbon in Metals (Thermodynamics, Kinetics and Properties).<br>Part XXII: Group Ib Metals (2): Silver, Gold.<br>H. Jehn W. Hehn, E. Fromm, G. Hörz |
| 2o-1 (1984) | Experimental Values of Critical Expoenents and Amplitude Ratios at Magnetic Phase Transitions.<br>K. Stierstadt, R. Anders, W. von Hörsten. |
| 27-1 (1983) | International Directory of Certified Radioactive Sources.<br>G. Grosse, W. Bambynek |

3. Bibliography of Existing Data Compilations

The bibliographic database "Physcomp" which covers data compilations in physics on a worldwide basis has been updated. A printed version will be published in the Physics Data series.

4. The Evaluated Nuclear Structure Data File (ENSDF)

The mass chain A = 98 has passed review procedure and is now in print. The mass chains A = 82, 94, 97 are nearly finished and will enter the review procedure in the next weeks. The work on the mass chains A = 81, 93 and 99 is going on.

The online retrievable databases ENSDF, MEDLIST, and NSR (Nuclear Structure Reference File) have been updated. In ENSDF, 62 mass chains have been replaced by their new versions. In the MEDLIST database, 533 radioactive decay data sets have been updated.

The bibliographic database "Nuclear Structure References" has been updated monthly. In all, app. 38oo new nuclear structure relevant documents have been added to the file.

# APPENDIX I

Addresses of Contributing Laboratories

Institut für Kernphysik II
Director: Prof. Dr. A. Citron
Senior reporter: Dr. S. Cierjacks
Kernforschungszentrum Karlsruhe
Postfach 3640
7500 Karlsruhe

Institut für Kernphysik III
Director: Prof. Dr. G. Schatz
Senior reporter: Dr. F. Käppeler
Kernforschungszentrum Karlsruhe
Postfach 3640
7500 Karlsruhe

Institut für Neutronenphysik und Reaktortechnik
Director: Prof. Dr. G. Kessler
Senior reporter: Dr. F.H. Fröhner
Kernforschungszentrum Karlsruhe
Postfach 3640
7500 Karlsruhe

Institut für Chemie (1): Nuklearchemie
Director: Prof. Dr. G. Stöcklin
Senior reporter: Dr. S.M. Qaim
Kernforschungsanlage Jülich
Postfach 1913
5170 Jülich

Institut für Reine und Angewandte Kernphysik
Director: Prof. Dr. K.O. Thielheim
Senior reporter: Dr. H.-G. Priesmeyer
Universität Kiel, Geesthacht
Reaktorstr. 1
2054 Geesthacht/Tesperhude

Institut für Physik
Director: Prof. Dr. W. Michaelis
Senior reporter: Dr. R. Pepelnik
GKSS-Forschungszentrum Geesthacht
2054 Geesthacht

Institut für Kernchemie
Senior reporter: Dr. R. Michel
Universität zu Köln
Zülpicher Str. 47
5000 Köln

Institut für Kernchemie
Director: Prof. Dr. G. Herrmann
Senior reporter: Prof. Dr. H.O. Denschlag
Universität Mainz
Fritz-Strassmann-Weg 2
6500 Mainz

Institut für Strahlenphysik
Director: Prof. Dr. K.W. Hoffmann
Senior reporter: J.W. Hammer
Universität Stuttgart
Allmandring 3
7000 Stuttgart 80

Fachbereich Physik der
Technischen Universität München
Abteilung E14, Forschungsreaktor
Head and senior reporter: Prof. Dr. L. Köster
8046 Garching/München

Institut für Kernchemie
Senior reporter: Prof. Dr. P. Patzelt
Philipps-Universität Marburg
Lahnberge
3550 Marburg/Lahn

Physikalisch-Technische Bundesanstalt
Abteilung 6, Atomphysik
Director: Prof. Dr. S. Wagner
Bundesallee 100
3300 Braunschweig

Fachinformationszentrum Energie, Physik, Mathematik
Directors: Drs. W. Rittberger, E.-O. Schulze
Senior reporter: Dr. H. Behrens
Kernforschungszentrum
7514 Eggenstein-Leopoldshafen 2

# APPENDIX II

## CINDA Type Index

Prepared by H. Behrens and G. Schust

FIZ Energie, Physik, Mathematik, Karlsruhe

| ELEMENT | QUANTITY | TYPE | ENERGY MIN | ENERGY MAX | DOCUMENTATION REF VOL PAGE | DATE | LAB | COMMENTS |
|---|---|---|---|---|---|---|---|---|
| MA NY | N,TRITON | EXPT-PROG | 30+7 | | NEANDC(E)-252U | 684 | JUL | VOL.5.P.19.QAIM+SIG SYSTEMATICS,GRPH |
| LI 007 | EVALUATION | EVAL-PROG | 28+6 | 16+7 | NEANDC(E)-252U | 684 | KFK | VOL.5.P.11.GOEL+ NNT SIG, GRAPH |
| LI 007 | N,N TRITON | EVAL-PROG | 26+6 | 16+7 | NEANDC(E)-252U | 684 | KFK | VOL.5.P.11.GOEL+ EVALUATED DATA, GRP |
| AL 027 | RESON PARAMS | EXPT-PROG | 35+4 | | NEANDC(E)-252U | 684 | KFK | VOL.5.P.4.WISSHAK+ WG, S-WAVE |
| CA 046 | N,GAMMA | EXPT-PROG | NDG | | NEANDC(E)-252U | 684 | KFK | VOL.5.P.4.KAEPPELER+ ABST, NDG |
| CA 048 | N,GAMMA | EXPT-PROG | NDG | | NEANDC(E)-252U | 684 | KFK | VOL.5.P.4.KAEPPELER+ ABST, NDG |
| TI 050 | N,PROTON | EXPT-PROG | 15+7 | | NEANDC(E)-252U | 684 | KIG | VOL.5.P.29.PEPELNIK+ TBL |
| CR 050 | N,GAMMA | EXPT-PROG | 15+7 | | NEANDC(E)-252U | 684 | KIG | VOL.5.P.29.PEPELNIK+ TBL |
| CR 050 | N,2N | EXPT-PROG | 15+7 | | NEANDC(E)-252U | 684 | KIG | VOL.5.P.29.PEPELNIK+ TBL |
| CR 052 | N,PROTON | EXPT-PROG | 15+7 | | NEANDC(E)-252U | 684 | KIG | VOL.5.P.29.PEPELNIK+ TBL |
| CR 052 | N,2N | EXPT-PROG | 15+7 | | NEANDC(E)-252U | 684 | KIG | VOL.5.P.29.PEPELNIK+ TBL |
| CR 053 | N,HELIUM3 | EXPT-PROG | 15+7 | | NEANDC(E)-252U | 684 | KIG | VOL.5.P.29.PEPELNIK+ TBL |
| CR 053 | N,N PROTON | EXPT-PROG | 15+7 | | NEANDC(E)-252U | 684 | KIG | VOL.5.P.29.PEPELNIK+ TBL |
| CR 053 | N,PROTON | EXPT-PROG | 15+7 | | NEANDC(E)-252U | 684 | KIG | VOL.5.P.29.PEPELNIK+ TBL |
| CR 054 | N,ALPHA | EXPT-PROG | 15+7 | | NEANDC(E)-252U | 684 | KIG | VOL.5.P.29.PEPELNIK+ TBL |
| CR 054 | N,PROTON | EXPT-PROG | 15+7 | | NEANDC(E)-252U | 684 | KIG | VOL.5.P.29.PEPELNIK+ TBL |
| MN 055 | N,ALPHA | EXPT-PROG | 15+7 | | NEANDC(E)-252U | 684 | KIG | VOL.5.P.29.PEPELNIK+ TBL |
| MN 055 | N,2N | EXPT-PROG | 15+7 | | NEANDC(E)-252U | 684 | KIG | VOL.5.P.29.PEPELNIK+ TBL |
| MN 055 | SCATTERING | THEO-PROG | NDG | | NEANDC(E)-252U | 684 | KFK | VOL.5.P.15.JAHN. DIFFSIG,NDG |
| FE 054 | N,ALPHA | EXPT-PROG | 15+7 | | NEANDC(E)-252U | 684 | KIG | VOL.5.P.29.PEPELNIK+ TBL |
| FE 054 | N,PROTON | EXPT-PROG | 15+7 | | NEANDC(E)-252U | 684 | KIG | VOL.5.P.29.PEPELNIK+ TBL |
| FE 054 | N,2N | EXPT-PROG | 15+7 | | NEANDC(E)-252U | 684 | KIG | VOL.5.P.29.PEPELNIK+ TBL |
| FE 056 | N,PROTON | EXPT-PROG | 15+7 | | NEANDC(E)-252U | 684 | KIG | VOL.5.P.29.PEPELNIK+ TBL |
| FE 056 | SCATTERING | THEO-PROG | 75+6 | 15+7 | NEANDC(E)-252U | 684 | KFK | VOL.5.P.15.JAHN. DIFFSIG,NDG |
| FE 056 | TOT | THEO-PROG | 20+5 | 50+5 | NEANDC(E)-252U | 684 | KFK | VOL.5.P.16.FROEHNER.S-WAVE SIG DISTR |
| FE 057 | N,N PROTON | EXPT-PROG | 15+7 | | NEANDC(E)-252U | 684 | KIG | VOL.5.P.29.PEPELNIK+ TBL |
| FE 057 | N,PROTON | EXPT-PROG | 15+7 | | NEANDC(E)-252U | 684 | KIG | VOL.5.P.29.PEPELNIK+ TBL |
| FE 058 | N,PROTON | EXPT-PROG | 15+7 | | NEANDC(E)-252U | 684 | KIG | VOL.5.P.29.PEPELNIK+ TBL |
| CO 059 | N,ALPHA | EXPT-PROG | 15+7 | | NEANDC(E)-252U | 684 | KIG | VOL.5.P.29.PEPELNIK+ TBL |
| CO 059 | N,PROTON | EXPT-PROG | 15+7 | | NEANDC(E)-252U | 684 | KIG | VOL.5.P.29.PEPELNIK+ TBL |
| CO 059 | N,2N | EXPT-PROG | 15+7 | | NEANDC(E)-252U | 684 | KIG | VOL.5.P.29.PEPELNIK+ TBL |
| NI 058 | N,ALPHA | EXPT-PROG | 50+6 | 15+7 | NEANDC(E)-252U | 684 | JUL | VOL.5.P.20.QAIM+ EXCIT FN, GRAPH |
| NI 058 | N,N PROTON | EXPT-PROG | 15+7 | | NEANDC(E)-252U | 684 | KIG | VOL.5.P.29.PEPELNIK+ TBL |
| NI 058 | N,PROTON | EXPT-PROG | 15+7 | | NEANDC(E)-252U | 684 | KIG | VOL.5.P.29.PEPELNIK+ TBL |
| NI 058 | N,2N | EXPT-PROG | 15+7 | | NEANDC(E)-252U | 684 | KIG | VOL.5.P.29.PEPELNIK+ TBL |
| NI 060 | N,PROTON | EXPT-PROG | 15+7 | | NEANDC(E)-252U | 684 | KIG | VOL.5.P.29.PEPELNIK+ TBL |
| NI 061 | N,PROTON | EXPT-PROG | 15+7 | | NEANDC(E)-252U | 684 | KIG | VOL.5.P.29.PEPELNIK+ TBL |
| NI 062 | N,ALPHA | EXPT-PROG | 50+6 | 15+7 | NEANDC(E)-252U | 684 | JUL | VOL.5.P.20.QAIM+ EXCIT FN, GRAPH |
| NI 062 | N,N PROTON | EXPT-PROG | 15+7 | | NEANDC(E)-252U | 684 | KIG | VOL.5.P.29.PEPELNIK+ TBL |
| NI 062 | N,PROTON | EXPT-PROG | 15+7 | | NEANDC(E)-252U | 684 | KIG | VOL.5.P.29.PEPELNIK+ TBL |
| NI 064 | N,ALPHA | EXPT-PROG | 50+6 | 15+7 | NEANDC(E)-252U | 684 | JUL | VOL.5.P.20.QAIM+ EXCIT FN, GRAPH |
| NI 064 | N,ALPHA | EXPT-PROG | 15+7 | | NEANDC(E)-252U | 684 | KIG | VOL.5.P.29.PEPELNIK+ TBL |
| NI 064 | N,N PROTON | EXPT-PROG | 15+7 | | NEANDC(E)-252U | 684 | KIG | VOL.5.P.29.PEPELNIK+ TBL |
| NI 064 | RESON PARAMS | EXPT-PROG | 14+4 | 34+4 | NEANDC(E)-252U | 684 | KFK | VOL.5.P.5.WISSHAK+ WG, S-WAVE |

| ELEMENT S A | QUANTITY | TYPE | ENERGY MIN | ENERGY MAX | DOCUMENTATION REF VOL PAGE DATE | LAB | COMMENTS |
|---|---|---|---|---|---|---|---|
| ZN | THERMAL SCAT | EXPT-PROG | 13+0 | | NEANDC(E)-252U 684 | MUN | VOL.5.P.46.KOESTER+ SCAT LENGTH+SIG |
| ZN 064 | THERMAL SCAT | EXPT-PROG | 13+0 | | NEANDC(E)-252U 684 | MUN | VOL.5.P.46.KOESTER+ SCAT LENGTH+SIG |
| ZN 066 | THERMAL SCAT | EXPT-PROG | 13+0 | | NEANDC(E)-252U 684 | MUN | VOL.5.P.46.KOESTER+ SCAT LENGTH+SIG |
| ZN 067 | THERMAL SCAT | EXPT-PROG | NDG | | NEANDC(E)-252U 684 | MUN | VOL.5.P.46.KOESTER+ COH SCAT LENGTH |
| ZN 068 | N,ALPHA | EXPT-PROG | 15+7 | | NEANDC(E)-252U 684 | KIG | VOL.5.P.29.PEPELNIK+ TBL |
| ZN 068 | N,PROTON | EXPT-PROG | 15+7 | | NEANDC(E)-252U 684 | KIG | VOL.5.P.29.PEPELNIK+ TBL |
| ZN 068 | THERMAL SCAT | EXPT-PROG | NDG | | NEANDC(E)-252U 684 | MUN | VOL.5.P.46.KOESTER+ COH SCAT LENGTH |
| GA | THERMAL SCAT | EXPT-PROG | 13+0 | 19+1 | NEANDC(E)-252U 684 | MUN | VOL.5.P.46.KOESTER+ SCAT LENGTH+SIG |
| GA 069 | THERMAL SCAT | EXPT-PROG | 13+0 | 52+0 | NEANDC(E)-252U 684 | MUN | VOL.5.P.46.KOESTER+ SCAT LENGTH+SIG |
| GA 071 | THERMAL SCAT | EXPT-PROG | NDG | | NEANDC(E)-252U 684 | MUN | VOL.5.P.46.KOESTER+ COH SCAT LENGTH |
| BR 079 | TOTAL | EXPT-PROG | 15+7 | | NEANDC(E)-252U 684 | KIG | VOL.5.P.29.PEPELNIK+ TBL |
| KR | N,GAMMA | EXPT-PROG | 30+3 | 24+5 | NEANDC(E)-252U 684 | KFK | VOL.5.P.6.WALTER+ ABST, NDG |
| ZR 090 | N,ALPHA | EXPT-PROG | 15+7 | | NEANDC(E)-252U 684 | KIG | VOL.5.P.29.PEPELNIK+ TBL |
| ZR 090 | N,PROTON | EXPT-PROG | 15+7 | | NEANDC(E)-252U 684 | KIG | VOL.5.P.29.PEPELNIK+ TBL |
| ZR 090 | N,2N | EXPT-PROG | 15+7 | | NEANDC(E)-252U 684 | KIG | VOL.5.P.29.PEPELNIK+ TBL |
| NB 093 | N,2N | THEO-PROG | 10+6 | 15+7 | NEANDC(E)-252U 684 | KFK | VOL.5.P.11.GOEL+ N-EMISS SPECT,GRAPH |
| NB 093 | SCATTERING | THEO-PROG | NDG | | NEANDC(E)-252U 684 | KF | VOL.5.P.15.JAHN. DIFFSIG,NDG |
| CD | TOTAL | EXPT-PROG | 24+4 | | NEANDC(E)-252U 684 | KIG | VOL.5.P.25.PRIESMEYER+ TBL |
| SB | THERMAL SCAT | EXPT-PROG | 13+0 | 52+0 | NEANDC(E)-252U 684 | MUN | VOL.5.P.46.KOESTER+ SCAT LENGTH+SIG |
| TE | THERMAL SCAT | EXPT-PROG | 13+0 | 52+0 | NEANDC(E)-252U 684 | MUN | VOL.5.P.46.KOESTER+ SCAT LENGTH+SIG |
| XE 124 | N,GAMMA | EXPT-PROG | 25+4 | | NEANDC(E)-252U 684 | KFK | VOL.5.P.6.BEER+ TBL |
| XE 128 | N,GAMMA | THEO-PROG | 30+4 | | NEANDC(E)-252U 684 | KFK | VOL.5.P.6.BEER+ STATMDL CALC, TBL |
| XE 129 | N,GAMMA | THEO-PROG | 30+4 | | NEANDC(E)-252U 684 | KFK | VOL.5.P.6.BEER+ STATMDL CALC, TBL |
| XE 130 | N,GAMMA | THEO-PROG | 30+4 | | NEANDC(E)-252U 684 | KFK | VOL.5.P.6.BEER+ STATMDL CALC, TBL |
| XE 131 | N,GAMMA | THEO-PROG | 30+4 | | NEANDC(E)-252U 684 | KFK | VOL.5.P.6.BEER+ STATMDL CALC, TBL |
| XE 132 | N,GAMMA | EXPT-PROG | 25+4 | | NEANDC(E)-252U 684 | KFK | VOL.5.P.6.BEER+ CFD CALC DATA, TBL |
| XE 134 | N,GAMMA | EXPT-PROG | 25+4 | | NEANDC(E)-252U 684 | KFK | VOL.5.P.6.BEER+ CFD CALC DATA, TBL |
| ND 142 | N,GAMMA | EXPT-PROG | NDG | | NEANDC(E)-252U 684 | KFK | VOL.5.P.7.MATHEWS+ S-PROCESS,ABST |
| ND 143 | N,GAMMA | EXPT-PROG | NDG | | NEANDC(E)-252U 684 | KFK | VOL.5.P.7.MATHEWS+ S-PROCESS,ABST |
| ND 144 | N,GAMMA | EXPT-PROG | NDG | | NEANDC(E)-252U 684 | KFK | VOL.5.P.7.MATHEWS+ S-PROCESS,ABST |
| SM 152 | N,GAMMA | EXPT-PROG | 25+4 | | NEANDC(E)-252U 684 | KFK | VOL.5.P.8.BEER+ MAXW AVG SIG, NDG |
| EU 151 | N,GAMMA | EXPT-PROG | 25+4 | | NEANDC(E)-252U 684 | KFK | VOL.5.P.8.BEER+ MAXW AVG SIG, NDG |
| GD 152 | N,GAMMA | EXPT-PROG | 25+4 | | NEANDC(E)-252U 684 | KFK | VOL.5.P.8.BEER+ MAXW AVG SIG, NDG |
| GD 158 | N,GAMMA | EXPT-PROG | 25+4 | | NEANDC(E)-252U 684 | KFK | VOL.5.P.8.BEER+ MAXW AVG SIG, NDG |
| GD 160 | N,GAMMA | EXPT-PROG | 25+4 | | NEANDC(E)-252U 684 | KFK | VOL.5.P.8.BEER+ MAXW AVG SIG, NDG |
| DY 162 | RESON PARAMS | EXPT-PROG | 54+0 | | NEANDC(E)-252U 684 | KIG | VOL.5.P.25.PRIESMEYER+ WN,RES-EN |
| ER 167 | TOTAL | EXPT-PROG | 15+7 | | NEANDC(E)-252U 684 | KIG | VOL.5.P.29.PEPELNIK+ TBL |
| ER 167 | TOTAL | EXPT-PROG | 15+7 | | NEANDC(E)-252U 684 | KIG | VOL.5.P.29.PEPELNIK+ TBL |
| ER 168 | N,2N | EXPT-PROG | 15+7 | | NEANDC(E)-252U 684 | KIG | VOL.5.P.29.PEPELNIK+ TBL |
| TM | POLARIZATION | EXPT-PROG | 76+6 | | NEANDC(E)-252U 684 | THS | VOL.5.P.43.BULSKI+ ANALYZ POWER,NDG |

| ELEMENT S A | QUANTITY | TYPE | ENERGY MIN | ENERGY MAX | DOCUMENTATION REF VOL PAGE DATE | LAB | COMMENTS |
|---|---|---|---|---|---|---|---|
| YB 174 | N,PROTON | EXPT-PROG | 15+7 | | NEANDC(E)-252U 684 | KIG | VOL.5.P.29.PEPELNIK+ TBL |
| YB 176 | TOTAL | EXPT-PROG | 15+7 | | NEANDC(E)-252U 684 | KIG | VOL.5.P.29.PEPELNIK+ TBL |
| TA | POLARIZATION | EXPT-PROG | 78+6 | | NEANDC(E)-252U 684 | THS | VOL.5.P.43.BULSKI+ ANALYZ POWER,NDG |
| W | POLARIZATION | EXPT-PROG | 78+6 | | NEANDC(E)-252U 684 | THS | VOL.5.P.43.BULSKI+ ANALYZ POWER,NDG |
| W 183 | TOTAL | EXPT-PROG | 15+7 | | NEANDC(E)-252U 684 | KIG | VOL.5.P.29.PEPELNIK+ TBL |
| W 184 | N,2N | EXPT-PROG | 15+7 | | NEANDC(E)-252U 684 | KIG | VOL.5.P.29.PEPELNIK+ TBL |
| OS 190 | TOTAL | EXPT-PROG | 15+7 | | NEANDC(E)-252U 684 | KIG | VOL.5.P.29.PEPELNIK+ TBL |
| OS 192 | TOTAL | EXPT-PROG | 15+7 | | NEANDC(E)-252U 684 | KIG | VOL.5.P.29.PEPELNIK+ TBL |
| IR 191 | TOTAL | EXPT-PROG | 15+7 | | NEANDC(E)-252U 684 | KIG | VOL.5.P.29.PEPELNIK+ TBL |
| AU | N,GAMMA | EXPT-PROG | NDG | | NEANDC(E)-252U 684 | KFK | VOL.5.P.9.WISSHAK+ SELF-ABS CORR,NDG |
| AU | TOTAL | EXPT-PROG | 24+4 | | NEANDC(E)-252U 684 | KIG | VOL.5.P.25.PRIESMEYER+ TBL |
| PB | TOTAL | EXPT-PROG | 24+4 | | NEANDC(E)-252U 684 | KIG | VOL.5.P.25.PRIESMEYER+ TBL |
| PB 206 | DIFF ELASTIC | EXPT-PROG | 78+6 | | NEANDC(E)-252U 684 | THS | VOL.5.P.43.BULSKI+ ANGDIST,GRAPH |
| PB 206 | POLARIZATION | EXPT-PROG | 78+6 | | NEANDC(E)-252U 684 | THS | VOL.5.P.43.BULSKI+ANALYZ POWER,GRAPH |
| PB 207 | TOTAL | EXPT-PROG | 15+7 | | NEANDC(E)-252U 684 | KIG | VOL.5.P.29.PEPELNIK+ TBL |
| PB 208 | N,2N | EXPT-PROG | 15+7 | | NEANDC(E)-252U 684 | KIG | VOL.5.P.29.PEPELNIK+ TBL |
| PB 208 | POLARIZATION | EXPT-PROG | 78+6 | | NEANDC(E)-252U 684 | THS | VOL.5.P.43.BULSKI+ ANALYZ POWER,NDG |
| TH | THERMAL SCAT | EXPT-PROG | 13+0 | 52+0 | NEANDC(E)-252U 684 | MUN | VOL.5.P.46.KOESTER+ SCAT LENGTH+SIG |
| TH 232 | POLARIZATION | EXPT-PROG | 78+6 | | NEANDC(E)-252U 684 | THS | VOL.5.P.43.BULSKI+ ANALYZ POWER,NDG |
| U 235 | FRAG CHARGE | EXPT-PROG | PILE | | NEANDC(E)-252U 684 | MNZ | VOL.5.P.38.DENSCHLAG+YIELD A=130-147 |